ADVERSARIALLY ROBUST ANOMALY DETECTION THROUGH SPURIOUS NEGATIVE PAIR MITIGATION

Anonymous authors
Paper under double-blind review

ABSTRACT

Despite significant progress in Anomaly Detection (AD), the robustness of existing detection methods against adversarial attacks remains a challenge, compromising their reliability in critical real-world applications such as autonomous driving. This issue primarily arises from the AD setup, which assumes that training data is limited to a group of unlabeled normal samples, making the detectors vulnerable to adversarial anomaly samples during testing. Additionally, implementing adversarial training as a safeguard encounters difficulties, such as formulating an effective objective function without access to labels. An ideal objective function for adversarial training in AD should promote strong perturbations both within and between the normal and anomaly groups to maximize margin between normal and anomaly distribution. To address these issues, we first propose crafting a pseudo-anomaly group derived from normal group samples. Then, we demonstrate that adversarial training with contrastive loss could serve as an ideal objective function, as it creates both inter- and intra-group perturbations. However, we notice that spurious negative pairs compromise the conventional contrastive loss for achieving robust AD. Spurious negative pairs are those that should be mapped closely but are erroneously separated. These pairs introduce noise and misguide the direction of inter-group adversarial perturbations. To overcome the effect of spurious negative pairs, we define opposite pairs and adversarially pull them apart to strengthen inter-group perturbations. Experimental results demonstrate our superior performance in both clean and adversarial scenarios, with a **26.1%** improvement in robust detection across various challenging benchmark datasets.

1 INTRODUCTION

Anomaly detection (AD), also referred to as one-class classification, aims to identify whether an input sample at the time of inference belongs to the normal[1] or anomaly group. In AD setup, the training data consists only of normal samples, and any additional information, such as labels, is unavailable (1; 2). Recently, a plethora of literature has emerged to address the problem of AD on images, demonstrating near-perfect performance on standard AD benchmarks (3–8). Nevertheless, these methods demonstrate a lack of robustness, especially when faced with adversarial attacks, as they encounter substantial performance deterioration when faced with such scenarios (9–16). This is due to the absence of anomaly samples in the training data, which results in insufficient exposure to adversarial perturbations on anomalous patterns during training. This shortcoming would make the model vulnerable to adversarial attacks on anomaly samples during inference (11; 16).

Numerous defense strategies have been developed to enhance the robustness of deep neural networks, with adversarial training emerging as a potential solution (17; 18). However, its application to AD is not straightforward, as it is primarily developed for multi-class and labeled setups.

Motivated by the aforementioned issues, we propose generating pseudo-anomaly group samples by applying hard augmentations to facilitate practical adversarial training in an anomaly detection (AD) setup. This process involves shifting normal training data to ensure that the shifted samples do not belong to the normal group, measured by their likelihood using a novel thresholding approach (19). We refer to the relationship between a normal sample and its transformed version as *opposite pairs*.

[1] In this study, the term '*normal distribution*' refers to inlier samples, not to Gaussian distribution.

Given the availability of two groups—crafted anomaly and normal samples—during training, defining a loss function to incorporate them into the adversarial training presents a new challenge. Since the objective of test-time adversarial attacks is to manipulate normal samples to be confused with anomalies and vice versa, the optimal objective function should maximize the margin between the distributions of normal and anomaly samples in the learned embedding space while also achieving compact representations for each group. This can be adversarially accomplished by crafting strong intra- and inter-group perturbations (20–22).

It has been demonstrated that Contrastive Learning (CL) (23; 24) is more effective for AD compared to existing objective functions (25; 26; 4). One can propose adversarial training with CL to develop a robust AD method. However, we noticed that adversarial training with the CL loss function falls short of achieving robust AD (see Table 6). The CL objective aims to bring positive pairs closer together and push negative pairs further apart. Positive pairs are constructed by applying light transformations to each instance, while any two instances in the training data are treated as negative pairs. We refer to negative pairs within the same group (normal-normal or anomaly-anomaly) as *spurious negative pairs*. These spurious negative pairs weaken the effectiveness of adversarial CL by misdirecting inter-group perturbations, thereby reduces the margin between groups (20).

To address this, we propose COBRA (anomaly-aware **CO**ntrastive-**B**ased approach for **R**obust **A**D), a new method that mitigates the effect of spurious negative pairs to learn effective perturbations. COBRA strategically utilizes opposite pairs, exclusively formed between normal and anomaly groups, ensuring they do not intersect with spurious negatives. This approach strengthens inter-group perturbations by emphasizing these opposite pairs in the loss function, thereby increasing the margin between groups. During training, the model adversarially targets positive pairs to push them together and opposite pairs to pull them apart. This simulates a wide range of adversarial perturbations covering inter- and intra-set variations, resulting in a robust anomaly detector.

Contribution. COBRA introduces a simple yet effective approach to generate anomaly samples and a novel loss function to establish a robust detection boundary. We evaluate COBRA in both adversarial and clean settings, where test samples are benign. In the adversarial scenario, we employ numerous strong attacks for robustness evaluation, including PGD-1000 (18), AutoAttack (27), and Adaptive AutoAttack (28). The results show that COBRA, without using any additional datasets or pretrained models, significantly outperforms existing methods in adversarial settings, achieving a 26.1% improvement in AUROC and competitive results in standard settings. Our experiments span various datasets, including large and real-world datasets such as Autonomous Driving (29), ImageNet (30), MVTecAD (7), and ISIC (31), demonstrating COBRA's practical applicability. Additionally, we conducted ablation studies to examine the impact of various COBRA components, specifically our pseudo-anomaly generation strategy and the introduced adversarial training method.

2 PRELIMINARIES

Anomaly Detection. Outlier detection is categorized into different areas, such as AD and Out-of-Distribution (OOD) detection, depending on the availability of normal set samples' labels. An AD method decides whether x belongs to the normal or anomaly set by assigning an anomaly score $A(x; f)$ using model f. Samples with an anomaly score higher than a pre-assumed threshold are predicted as anomalies, and vice versa (32; 33). It is important to note that extending OOD detection methods to an AD setup is not feasible, as they rely on labeled normal data for feature extraction. This highlights the need for robust AD methods.(9; 16; 34; 35).

Adversarial Robustness of Anomaly Detectors. An adversarial attack, which is primarily explored for classification tasks, is a malicious attempt to perturb a data sample x with an associated label y into a new sample x^* that maximizes the loss function $\ell(x^*; y)$. Consequently, x^* is termed an adversarial example of x, and the disparity (x^* - x) is termed adversarial perturbation. Additionally, an upper limit of ϵ confines the l_p norm of the adversarial noise to prevent semantic alterations. Specifically, an adversarial example x^* must satisfy the following equations: $x^* = \arg\max_{x':\|x-x'\|_p \leq \epsilon} \ell(x'; y)$ A prevalent and effective attack method is the Projected Gradient Descent (PGD) technique (18), which entails iteratively maximizing the loss function by advancing towards the gradient sign of $\ell(x^*; y)$, employing a designated step size α. To adapt adversarial attacks for AD, instead of maximizing the loss value, we aim to increase $A(x, f)$ if x belongs to normal group and decrease it otherwise. The formulation of the attack would be: $x_0^* = x, \quad x_{t+1}^* = x_t^* + y \cdot \alpha \cdot \operatorname{sign}\left(\nabla_x A(x_t^*; f_\theta)\right), \quad x^* = x_k^*$

where $y = +1$ for normal samples and $y = -1$ for anomaly samples. The same setting is applied to other attacks in our study.

Auxiliary Anomaly Sample Crafting. CSI (4) and CPAD (36) propose using fixed hard augmentation to create auxiliary samples. Specifically, CSI relies on Rotation, while CPAD considers CutPaste as a pseudo-anomaly. The GOE (37) method employs a pretrained GAN on ImageNet-1K to craft anomalies by targeting low-density areas. FITYM (38) employed an underdeveloped diffusion as a generator. Dream-OOD (39) uses both image and text domains to learn visual representations of normal instances in an embedding space of a pretrained stable diffusion (40) model trained on 5 billion data (e.g. LAION (41)). On the other hand, VOS (42) generates anomaly embeddings instead of image data. Details about each mentioned method can be found in Appendix C.

3 METHOD

Motivation. Adversarial training is one of the most promising approaches to enhance the robustness of deep neural networks. However, applying this technique to AD poses a significant challenge, as only a single concept class—the normal distribution—is available during training. A common approach to address this limitation is to incorporate an auxiliary anomaly dataset to improve robustness (9; 16; 11; 43). However, leveraging such datasets is both costly and challenging, primarily due to the need for preprocessing and filtering out normal samples, which could otherwise provide misleading information to the detector. Moreover, the use of additional anomaly data can bias the model towards specific anomaly samples, reducing its generalizability to unseen anomalies (44).

To overcome these limitations, we propose a simple yet effective method to craft anomaly samples directly from the normal data, thus eliminating the need for external anomaly datasets. Our approach involves applying hard augmentations (e.g., severe distortions) to normal samples, effectively pushing them towards the anomaly distribution. Importantly, prior work has demonstrated that the most effective anomalies for training are those that are closely related to the normal distribution, often referred to as "near anomaly samples" (38; 16). Our method satisfies this proximity, as the crafted anomalies maintain stylistic similarities with the normal samples due to their generation through augmentations.

To ensure that the crafted anomalies have sufficiently shifted away from the normal distribution, we introduce a thresholding mechanism to filter out false anomalies. Specifically, we use a simple unsupervised model to extract meaningful representations from the crafted samples and filter those that remain too close to the normal distribution (45; 46). Subsequently, we explore potential objective functions for adversarial training, focusing on CL given its recent success in AD tasks (25).

However, we observe that employing standard CL in adversarial training may not yield optimal results. This stems from the fact that, when training on a dataset containing both normal and crafted anomaly samples, CL forms positive and negative pairs in a way that may compromise the margin between the normal and anomaly distributions. Specifically, CL seeks to uniformly repel negative pairs from each other, defined as all pairs except those that are augmentations of each other (47). Consequently, the negative pairs include normal-normal, anomaly-anomaly, and normal-anomaly pairs. Increasing the distance between normal-normal and anomaly-anomaly pairs may inadvertently reduce the separation between normal and anomaly sets, thus undermining robust detection performance. In other words, standard CL does not effectively enhance the inter-set margin needed to improve robustness.

To address this, we design a novel objective function that explicitly maximizes the margin between the normal and anomaly groups to improve inter-group perturbation. Our approach introduces "opposite pairs"—a subset of negative pairs consisting solely of normal-anomaly pairs—and explicitly repels these pairs to maximize the margin between the normal and anomaly distributions. We utilize this loss function in conjunction with adversarial training using PGD-10 (l_∞) to strengthen the model's robustness.

Outline. Existing AD methods experience dramatic performance decrease under adversarial attack. To address this, we propose COBRA, a novel method that integrates a distribution-aware transformation for generating psudo-anomaly samples, coupled with a novel objective function for adversarial training. In the subsequent sections, we will delve into each component in detail, outlining the mechanisms and advantages of our approach.

3.1 DISTRIBUTION AWARE HARD TRANSFORMATION

Anomaly Crafting Strategy. Previous works have demonstrated the effectiveness of leveraging an auxiliary random dataset as an additional source of anomaly data during the training phase for AD (48; 49; 42; 39; 50; 38; 37). However, this technique significantly depends on the diversity and distribution distance of the auxiliary dataset used for training. This limitation significantly hinders the use of this technique in areas like medical imaging, where real anomalies are scarce and difficult to obtain. Moreover, they lack any threshold for dropping incorrectly crafted anomalies (those that still belong to the normal group). Addressing this limitation, our approach introduces a novel method that employs a series of hard transformations $T = \{T_i\}_{i=1}^{k}$ to generate anomaly samples from normal data. We strategically distort normal images and by using a predetermined threshold ensures that the synthetically created samples significantly diverge from the normal distribution.

We used a set of hard transformations including Jigsaw (51), Random Erasing (52), CutPaste (53), Rotation, Extreme Blurring, Intense Random Cropping, Noise Injection (54), and Extreme Cropping, Mixup (55), Cutout (56), CutMix (57), Elastic transform and etc. Each one has been shown to be harmful for preserving semantics in previous studies (4; 58–61; 36; 62–66). For more details, please see Appendix D.1.

Threshold Computing. The insight behind our threshold is to estimate the boundary of the normal distribution by computing low-likelihood regions (42). By doing so, we aim to reject any crafted samples that exhibit a higher likelihood than this threshold, ensuring that only genuine anomalies are considered. In the first step, our goal is to develop a model that learns meaningful representations from the normal distribution and to define a threshold based on those representations. Inspired by (45; 46; 4), we train a transformation predictor model that captures the distribution of normal samples through the classification of various augmentations.

We create a synthetic dataset with k classes, $\{D_{\text{train}}^{T_i}\}_{i=1}^{k}$, by applying k different hard transformations T_i to each of the n samples in the normal training set D_{train}. We then train a k-class Resnet18 classifier on this synthetic dataset to leverage the classifier's knowledge for threshold computing. Using the classifier as a feature extractor, denoted as C, we extract embeddings of normal training samples to create an embedding set $e_{\text{train}} = \left\{C(D_{\text{train}}^{i})\right\}_{i=1}^{n}$. Next, we fit a Gaussian Mixture Model (GMM) to the training data embeddings e_{train}, as this is a well-supported approach in the literature (67; 42). We compute the likelihood for each sample and then calculate the **p-value** for test samples based on the empirical distribution of likelihoods from the normal training samples. The threshold λ is set at a default significance level of 0.05, such that samples with p-values below this threshold are considered anomalies. An ablation study on the significance level, as well as an analysis of C, are provided in Appendix D and Appendix E, respectively.

Opposite Pairs with Pseudo-Anomaly Samples. For each normal sample, we randomly select a subset of transformations T, containing at least two transformation. These transformations are applied in a randomized sequence to the sample, producing $x' = T_{i_m}(\dots T_{i_1}(x))$ where $m < k$. We then get its embedding and calculate the likelihood $pr(C(x'))$. Finally, this likelihood is compared against a threshold λ. Samples exceeding this threshold iteratively repeat this process until deemed an anomaly. We represent our proposed strategy for anomaly crafting with the notation $\Upsilon(x)$. Before each step of training, given a batch of normal samples denoted by $\mathcal{B}_{\text{normal}} = \{x^j\}_{j=1}^{b}$, we create a batch of anomaly samples $\mathcal{B}_{\text{p-anomaly}} = \{x^j\}_{j=b+1}^{2b}$. Where $x^{b+i} = \Upsilon(x^i)$ signifies an anomaly sample derived from applying a transformation Υ to a normal sample x^i, and (x^i, x^{b+i}) are considered as symmetrically opposite pairs. During training, the notation $\Upsilon(x)$ has some minor differences, where $\Upsilon(x^{b+i})$ is considered as x^b.

3.2 ADVERSARIAL TRAINING WITH ANOMALY-AWARE CL

Conventional Contrastive Loss. In the conventional CL paradigm, each instance x within a batch transforms into two positive views, (x_1, x_2), via a random selection of positive augmentations τ_1, τ_2 from a predefined set $\mathcal{T}$. The set of positive pairs corresponding to a sample x is denoted as $\text{P}(x_1) = \{x_2\}$ and $\text{P}(x_2) = \{x_1\}$. CL then defines negative pairs $N(x)$ for sample x as the other samples' augmented views. By denoting the current batch as B, we achieve: $N(x) = \{\tau_1(x') : x' \in B \setminus \{x\}\} \cup \{\tau_2(x') : x' \in B \setminus \{x\}\}$. These views are processed through a target

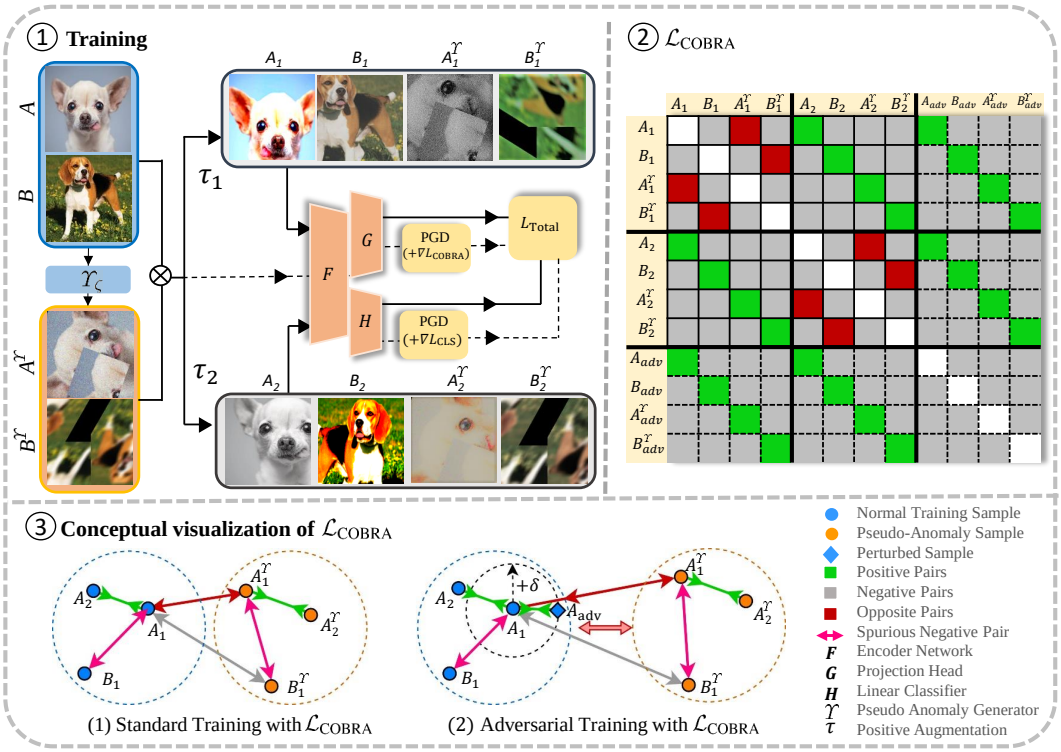

Figure 1: ①: Given a training batch that includes normal group samples A and B, we create a anomaly group using our proposed transformation Υ_λ. These samples are paired as opposite pairs (e.g., A and A^Υ) and subjected to augmentations τ_1 and τ_2 to form batches of positive pairs. Adversarial training is performed with a loss function combining L_{CLS} and L_{COBRA}, where L_{COBRA} treats adversarial examples as positive pairs for the corresponding sample. ②, ③: The illustrations demonstrate how L_{COBRA} enhances adversarial training by explicitly increasing similarities within positive pairs and decreasing similarity for opposite pairs, thus creating strong inter- and intra-group perturbations. Targeting opposite pairs instead of all negatives diminishes the effect of spurious negative pairs (e.g., (A_1, B_1)), leading to stronger inter-group perturbations and enlarging the margin between distributions for normal and anomaly groups. A detailed algorithmic of COBRA is provided in Appendix A.

network to obtain projected features, symbolized as $z = \mathcal{G}(\mathcal{F}(x))$, where $\mathcal{F}$ signifies the feature encoder and $\mathcal{G}$ the projection head. For simplification, $f(.)$ substitutes $\mathcal{G}(\mathcal{F}(.))$. The conventional NT-Xent (23) loss is articulated as:

$$\mathcal{L}_{\text{CL}}(x) = -\sum_{i=1}^{2} \sum_{x_j \in \text{P}(x_i)} \log \frac{\exp(\text{sim}(f(x_i), f(x_j))/t)}{\sum_{x_k \in \text{P}(x_i) \cup \text{N}(x)} \exp(\text{sim}(f(x_i), f(x_k))/t)}. \tag{1}$$

where $\text{sim}(\cdot, \cdot)$ denotes the cosine similarity function, t is the temperature parameter, $\text{P}(x_i)$ is the set of positive pairs for x_i, and $\text{N}(x_i)$ is the set of negative pairs for x_i.

Addressing Spurious Negative Pairs with $\mathcal{L}_{\text{COBRA}}$. CL aims to pull positive pairs closer to each other and push negative pairs away from each other. Consider defining the current batch of samples for CL as the concatenation of two groups: normal and anomaly samples, $\mathcal{B} = \{\mathcal{B}_{\text{normal}} \cup \mathcal{B}_{\text{p-anomaly}}\}$. Due to the definition of negative pairs in CL, each sample in $\mathcal{B}$ includes both inter-group and intra-group relations as negative pairs. Intra-group negative pairs, i.e., normal-normal and anomaly-anomaly pairs, are considered spurious negative pairs. Distancing spurious negative pairs is counterproductive to our objective, which is to maximize the discriminative margin between normal and anomaly groups. Specifically, in the scenario of adversarial training for robust AD with $\mathcal{L}_{\text{CL}}$, spurious negative pairs misdirect inter-group adversarial perturbation. As a result, we aim to precisely target those negative pairs that definitively belong to separate groups—what we refer to as opposite pairs. By focusing

on these pairs, we aim to induce stronger perturbations that significantly enhance the discriminative margin between the normal and anomaly groups by proposing $\mathcal{L}_{\text{COBRA}}$.

$$\mathcal{L}_{\text{COBRA}}(x) = -\sum_{i=1}^{2} \sum_{x_j \in \text{P}(x_i)} \log \frac{\exp(\text{sim}(f(x_i), f(x_j))/t) - \exp(\text{sim}(f(x_i), f(\Upsilon(x)))/t)}{\sum\limits_{x_k \in \text{P}(x_i) \cup \text{N}(x)} \exp(\text{sim}(f(x_i), f(x_k))/t)}, \quad (2)$$

The intuition behind $\mathcal{L}_{\text{COBRA}}$ is that the representations of the corresponding positive views x_1 and x_2 should be similar (analogous to the $\mathcal{L}_{\text{CL}}$ loss function), leading to compact representations for each group. Meanwhile, the representation of x should be distinctly different from its counterpart representation $\Upsilon(x)$, resulting in a high margin between the two groups. A conceptual visualization of $\mathcal{L}_{\text{COBRA}}$ is provided in Figure 1. It is important to highlight that the limitations of CL in AD are apparent in adversarial scenarios. This stems from the fact that adversarial training requires a higher degree of data complexity (68; 69) compared to clean settings, necessitating a broad range of strong perturbations to achieve robust anomaly detection. One can say $\mathcal{L}_{\text{COBRA}}$ consists of two terms, $\mathcal{L}_{\text{CL}}$ and $\mathcal{L}_{\text{Opposite}}$, where

$$\mathcal{L}_{\text{Opposite}}(x) = -\sum_{i=1}^{m} \sum_{x_j \in \text{P}(x_i)} \log \frac{-\exp(\text{sim}(f(x_i), f(\Upsilon(x))/t)}{\sum\limits_{x_k \in \text{P}(x_i) \cup \text{N}(x_i)} \exp(\text{sim}(f(x_i), f(x_k))/t)}, \quad (3)$$

To enhance our model's ability to distinguish between normal and anomaly groups, we employ a fully connected layer followed by softmax activation for binary classification, denoted as $\mathcal{H}$, following the $\mathcal{F}$. For the classification loss, $\mathcal{L}_{\text{CLS}}(x)$, we define a label y corresponding to the batch $\mathcal{B}$, where '0' is assigned as the label for normal samples and '1' for pseudo anomaly samples. Our final loss function, $\mathcal{L}_{\text{COBRA}}$, is thus formulated as: $\mathcal{L} = \sum_{i=1}^{2b} \mathcal{L}_{\text{COBRA}}(\mathcal{F}, \mathcal{G}; \mathcal{B}^i) + \mathcal{L}_{\text{CLS}}(\mathcal{F}, \mathcal{H}; \mathcal{B}^i, y^i)$

Adversarial Training Step. For $\mathcal{L}_{\text{COBRA}}$, given an input sample x from the batch $\mathcal{B}$, an adversarial example x_{adv} is generated by introducing a perturbation δ^*, optimized to maximize our final loss: $\delta^* = \underset{\|\delta\|_\infty \leq \epsilon}{\text{argmax}}\, \mathcal{L}(x + \delta^*, y), \quad x_{adv} = x + \delta^*$. Then, adversarial examples are used in the training process alongside the original examples. Specifically, for $\mathcal{L}_{\text{COBRA}}$, we consider them as another positive view of each sample and aim to align each sample with its perturbed version, i.e., $P(x_i) \leftarrow P(x_i) \cup \{x_{adv}\}$. The adversarial training objective as a min-max problem, optimizing the model parameters θ to minimize the expected loss over both clean and adversarial examples:

$$\min_{\theta} \mathbb{E}_{(x,y)\in\mathcal{B}} \left[\max_{\|\delta\|_\infty \leq \epsilon} \mathcal{L}(x + \delta, y; \theta) \right].$$

Morever, the stability of the $\mathcal{L}_{\text{COBRA}}$ can be observed in both clean and adversarial training scenarios, as illustrated in the Appendix F.

Anomaly Score for Evaluation. For evaluating anomalies, we leverage the representation learned by $\mathcal{F}$ to compute the anomaly score, based on the similarity between test samples and normal training samples in the embedding space. The anomaly score $A(X)$ for a test sample x is defined as: $-\max_{x^i \in D_{\text{train}}} \left\{ sim(f(\mathbf{x}), f(\mathbf{x}^i) \right\}$, This scoring mechanism takes advantage of the contrastive training framework, ensuring that normal test samples exhibit higher similarity scores in comparison to anomaly test samples. Consequently, the anomaly score for anomaly test samples will be notably higher than for normal test samples, enabling robust AD. Alternative anomaly scores have been explored in the appendix E.

4 EXPERIMENTS

In this section, we verify the effectiveness of COBRA in robust AD with several benchmark datasets, encompassing those that are large-scale and real-world. Evaluation is conducted to assess existing AD methods, including both clean and adversarially trained approaches, as well as our own method, under both clean and various adversarial attack scenarios. Table 1 provides a comparative analysis in a one-class setting 4 on the MVTecAD dataset, a challenging real-world benchmark in AD. Additional comparisons in one-class settings across other benchmarks are detailed in Table 2, while Table 3 showcases our method's superiority in unlabeled multi-class setting 4. Moreover, we demonstrate our method's robustness by evaluating it against several attacks presented in Table 4. Additional details

Table 1: Performance of AD methods on MVTecAD dataset under clean evaluation and PGD-1000 adversarial attack with $\epsilon = \frac{2}{255}$, measured by AUROC (%). The best results are emphasized in bold format in each row. The table cells denote results in the 'Clean / PGD-1000' format.

*These works incorporated adversarial training into their proposed AD methods.

Category	Method								
	CSI	Transformaly	PatchCore	ReContrast	DRÆM	PrincipaLS*	OCSDF*	ZARND*	COBRA (Ours)
Carpet	50.2 / 11.1	95.5 / 0.0	98.7 / 18.4	99.8 / 9.4	97.0 / 0.0	54.8 / 33.6	56.1 / 12.6	**85.9** / 66.6	60.7 / **84.9**
Grid	71.2 / 8.3	84.2 / 7.8	98.2 / 11.7	100.0 / 19.8	99.9 / 2.7	72.1 / 30.4	61.7 / 17.3	75.7 / 31.1	**100.0** / **99.5**
Leather	70.9 / 0.4	99.9 / 4.1	100.0 / 10.5	100.0 / 3.4	**100.0** / 0.0	73.2 / 26.5	61.4 / 13.7	65.0 / 14.1	97.4 / **91.7**
Tile	67.8 / 7.2	97.1 / 2.0	98.7 / 4.6	99.8 / 2.4	99.6 / 0.0	58.7 / 26.3	54.3 / 10.1	**53.6** / 3.9	98.8 / **78.2**
Wood	71.3 / 6.0	98.5 / 0.0	99.2 / 3.8	99.0 / 1.6	99.1 / 1.8	67.3 / 31.2	63.9 / 3.7	**58.4** / 17.5	96.4 / **73.7**
Bottle	69.4 / 1.2	99.4 / 5.1	100.0 / 9.4	100.0 / 6.8	99.2 / 2.1	72.1/ 29.4	59.8 / 9.1	79.9/ 54.9	**100.0** / **88.8**
Cable	66.5 / 7.9	81.5 / 0.1	99.5 / 4.3	99.8 / 3.3	91.8 / 1.9	63.9 / 26.2	61.6 / 6.3	**68.5** / 30.0	92.4 / **74.8**
Capsule	51.6 / 6.8	76.0 / 0.0	98.1 / 3.1	97.7 / 2.7	98.5 / 0.0	56.8 / 18.4	51.9 / 1.9	**69.3** / 26.2	75.9 / **55.8**
HazelNut	66.7 / 0.0	89.8 / 0.4	100.0 / 7.8	100.0 / 4.1	**100.0** / 0.8	64.8 / 21.7	54.2 / 4.7	73.2 /24.0	96.3 / **74.7**
MetalNut	65.8 / 0.7	90.9 / 6.2	100.0 / 4.8	**100.0** / 3.7	98.7 / 0.6	61.6 / 19.4	59.5 / 3.5	43.1 / 1.3	96.8 / **78.1**
Pill	48.3 / 3.1	83.7 / 2.0	96.6 / 2.0	98.6 / 1.8	98.9 / 0.0	52.5 / 9.4	57.4 / 0.7	**84.0** / 42.9	57.7 / **53.2**
Screw	51.7 / 0.0	73.3 / 0.4	**98.1** / 0.0	/ 98.0 / 3.8	93.9 / 0.0	57.6 / 3.7	55.0 / 0.6	84.7 / 21.4	74.2 / **36.4**
Toothbrush	75.3 / 1.3	90.8 / 0.9	100.0 / 6.9	100.0 / 6.7	100.0 / 0.0	70.8 / 28.2	60.1 / 6.4	65.9 / 22.3	**100.0** / **75.5**
Transistor	61.7 / 9.8	76.4 / 2.5	**100.0** / 7.8	99.7 / 8.1	93.1 / 5.3	60.1 / 26.3	58.7 / 4.5	86.5 / 46.3	91.0 / **69.2**
Zipper	68.2 / 5.4	90.7 / 0.8	99.4 / 13.6	99.5 / 13.7	**100.0** / 4.7	67.9 / 35.7/	65.6 / 9.8	82.2 /48.6	99.2 / **92.5**
Average	63.8 / 4.6	88.5 / 2.2	99.1 / 7.2	**99.5** / 6.1	98.0 / 1.3	63.6 / 24.4	58.7 / 7.0	71.6/ 30.1	89.1 / **75.1**

Table 2: Performance of AD methods on various datasets under clean evaluation and PGD-1000. For the experiments across **all tables**, adversarial attacks were considered, using $\epsilon = \frac{4}{255}$ for low-resolution images and $\epsilon = \frac{2}{255}$ for high-resolution images, measured by AUROC (%). The table cells denote results in the 'Clean / PGD' format. Experiments performed in the one-class AD setup.

*These works incorporated adversarial training into their proposed AD methods.

	Dataset	Method									
		DeepSVDD	CSI	MSAD	Transformaly	PatchCore	PrincipaLS*	OCSDF*	APAE*	ZARND*	COBRA (*Ours*)
Low Res	CIFAR10	64.8 / 8.7	94.3 / 10.6	97.2 / 4.8	**98.3** / 3.7	68.3 / 3.9	58.3 / 33.2	58.7 / 31.3	56.3 / 2.2	89.7 / 56.0	83.7 / **62.3**
	CIFAR100	67.0 / 3.6	89.6 / 11.9	96.4 / 8.4	**97.3** / 9.4	66.8 / 4.3	51.9 / 26.2	50.2 / 23.5	53.1 / 4.1	88.4 / 47.6	76.9 / **51.7**
	MNIST	94.8 / 8.2	93.8 / 3.4	96.0 / 3.2	94.8 / 7.9	83.2 / 2.6	97.8 / 83.1	96.1 / 68.9	93.4 / 34.7	**99.0** / 91.2	92.8 / **96.4**
	FMnist	94.5 / 7.9	92.7 / 5.8	94.2 / 6.6	94.4 / 7.4	77.4 / 5.5	92.5 / 69.2	91.8 / 64.9	88.3 / 19.5	**95.0** / 82.3	93.1 / **89.6**
	SVHN	60.3 / 1.5	**96.8** / 3.1	58.3 / 0.2	56.9 / 0.9	52.1 / 2.1	63.0 / 11.2	58.1 / 9.7	52.6 / 1.4	53.5 / 9.6	89.3 / **58.2**
High Res	ImageNet	56.4 / 4.0	91.6 / 5.6	98.9 / 2.6	**99.0** / 2.9	67.6 / 2.5	56.2 / 28.3	55.3 / 25.8	58.3 / 2.1	96.4 / 27.4	85.2 / **57.0**
	VisA	53.6 / 1.8	62.5 / 0.3	84.1 / 4.6	85.5 / 0.0	**95.1** / 2.7	57.3 / 16.1	53.0 / 13.9	67.2 / 9.1	71.8 / 24.9	75.2 / **73.8**
	CityScapes	59.7 / 2.7	68.9 / 0.1	86.5 / 2.9	87.4 / 4.5	**76.2** / 6.1	60.3 / 24.2	59.6 / 20.1	63.0 / 3.6	75.9 / 28.6	81.7 **56.2**
	DAGM	57.3 / 2.7	74.5 / 1.6	73.8 / 0.0	81.4 / 0.5	**93.6** / 1.9	59.2 / 24.8	57.6 / 20.3	54.5 / 13.8	64.5 / 17.2	82.4 / **56.8**
	ISIC2018	64.1 / 0.3	71.2 / 0.0	76.7 / 3.4	**86.6** / 3.9	78.9 / 0.0	61.7 / 26.5	64.0 / 18.6	67.2 / 8.5	70.2/ 14.6	81.3 / **56.1**
	Average	67.3 / 4.1	83.6 / 4.2	86.2 / 3.7	**88.1** / 4.1	75.9 / 3.1	65.8 / 34.3	64.5 / 29.7	65.4 / 9.9	80.4 /39.7	84.1 / **65.8**

on the adaptation of attacks and supplementary evaluation metrics can be found in Appendices K and N, respectively.

Analyzing Results. The results presented underscore COBRA's effectiveness as an robust AD method. Remarkably, COBRA enhances the average robust detection performance across various datasets by up to **26.1%**, **without** relying on pre-trained models or extra datasets. This demonstrates COBRA's real-world applicability by enhancing robust performance on the MVTecAD dataset from **30.1%** to **75.1%**. COBRA's versatility is further highlighted by its general applicability to different AD scenarios, including one-class and unlabeled multi-class setups. Notably, in open-world applications where robustness is vital, a slight drop in clean performance is considered a worthwhile trade-off for enhanced robustness. Our results align with this perspective, achieving an average of **84.1%** in clean and **65.8%** in adversarial settings across various datasets. This performance surpasses methods like Transformaly (67), which, while achieving 88.2% in clean settings, significantly falls to 4.1% in adversarial scenarios. Furthermore, we replaced our adversarial training with clean training in the

Table 3: Performance of AD methods under clean evaluation and PGD-1000, measured by AUROC (%). The table cells denote results in the 'Clean / PGD' format. Experiments performed in the unlabeled multi-class AD setup.

*These works incorporated adversarial training into their proposed AD methods.

In	Out	Method						
		MSAD	Transformaly	PrincipaLS*	OCSDF*	APAE*	ZARND*	COBRA (*Ours*)
CIFAR10	CIFAR100	76.9 / 0.4	88.7 / 0.0	54.8 / 14.6	51.0 / 12.8	53.6 / 1.2	76.6 / 34.1	76.0 / **63.3**
	SVHN	94.6 / 0.0	98.2 / 1.2	72.1 / 23.6	67.7 / 18.8	60.8 / 2.1	84.3 / 42.7	98.5 / **78.6**
	MNIST	99.3 / 1.6	99.4 / 3.6	82.5 / 42.7	74.2 / 37.4	71.3 / 15.3	99.4/ 82.2	80.8 / **85.8**
	FMnist	99.2 / 3.8	99.1 / 3.7	78.3 / 38.5	64.5 / 33.7	59.4 / 9.4	98.2/ 67.3	82.8 / **75.7**
	ImageNet	83.7 / 0.0	92.8 / 0.8	55.3 / 12.3	52.8 / 10.2	56.1 / 0.3	71.5 / 28.4	85.5 / **53.1**
CIFAR100	CIFAR10	61.4 / 0.0	82.5 / 0.3	47.6 / 8.1	51.1 / 6.3	50.5 / 0.7	64.6 / 21.2	48.7 / **27.5**
	SVHN	86.6 / 2.7	94.7 / 2.6	66.3 / 13.2	58.7 / 9.2	58.1 / 1.1	70.0/ 26.8	93.2 / **49.4**
	MNIST	97.4 / 3.5	98.8 / 0.8	80.4 / 30.4	76.4 / 28.9	74.7 / 11.8	87.0 / 30.4	77.8 / **54.1**
	FMnist	96.5 / 0.9	98.4 / 5.2	72.7 / 18.7	62.8 / 14.3	60.9 / 9.7	97.3 / **76.3**	58.2 / 32.9
	ImageNet	71.6 / 1.6	80.4 / 2.0	51.6 / 6.3	48.9 / 5.4	52.7 / 0.1	71.6 / 21.8	69.1 / **32.3**

Table 4: Performance of COBRA on various datasets under clean evaluation and several adversarial attack, measured by AUROC (%). Experiments performed in the one-class AD setup.

Dataset	Attack						
	Clean	BlackBox	FGSM	CAA	A^3	AutoAttack	PGD-1000
CIFAR10	83.7	81.8	70.2	64.5	60.7	65.9	62.3
CIFAR100	76.9	74.6	64.5	53.0	50.1	54.8	51.7
FMnist	93.1	92.9	90.7	91.6	90.8	87.4	89.6
ImageNet	85.2	82.0	71.4	53.6	61.8	59.4	57.0
MVTecAD	89.1	83.4	79.8	76.3	74.8	77.0	75.1
VisA	75.2	74.6	74.0	73.5	71.6	74.9	73.8

COBRA Pipeline. As expected, and in line with findings reported in the literature (70), this resulted in decreased robust detection performance. However, it improved clean detection performance from an AUROC of 84.1% to **90.7%**.

Experimental Setup. Our experiments were conducted in two categories: one-class and unlabeled multi-class anomaly detection (AD). In the one-class setup, considering a dataset D with M classes, experiments were conducted by treating each class in turn as the normal set and the other $M-1$ classes as the anomaly set. This process was repeated for each class, and performance was averaged across all classes to report the overall detection performance. In the unlabeled multi-class setup, this setting incorporates another dataset D', considering one dataset as the normal set and another as the anomaly set. We compared COBRA with PANDA (6), Transformaly (67), Patchcore (71), CSI (4), MSAD (26), ReContrast (25), and Draem (72), as well as methods specifically proposed for robust AD, including ZARND (73), PrincipaLS (10), OCSDF (14), and APAE (15). Details about each mentioned method can be found in Appendix C.

Evaluation Details. To evaluate the methods' adversarial robustness, both normal and anomalous test samples will be subjected to end-to-end adversarial attacks targeting the methods' anomaly scores. We set the value of ϵ to $\frac{4}{255}$ for low-resolution datasets and to $\frac{2}{255}$ for high-resolution datasets. For the PGD attack, we set the number of steps N to 1000, initializing the attack from 10 different random starting points for each trial to enhance the attack's effectiveness and coverage. Furthermore, to highlight COBRA's robust performance, we considered additional strong attacks, including AutoAttack (AA), Adaptive AutoAttack (A^3), and black-box attacks. Furthermore, to highlight COBRA's robust performance, we considered an additional range of simple to strong attacks, including black-box attacks (74), FGSM attacks (75), CAA (76), AutoAttack (AA), and Adaptive AutoAttack (A^3). Other methods' performance under AutoAttack can be found in Appendix G. Additionally, details on the model's evaluation under both ℓ_∞ and ℓ_2 PGD attacks across varying epsilon values are presented in Appendix H.

Implementation Details & Datasets For obtaining the threshold λ, we utilized a from-scratch ResNet-18 as C and trained on the created dataset for 100 epochs. For adversarial training, we use PGD-10 step and $\epsilon = \frac{4}{255}$. We employ ResNet-18 as the foundational encoder network, accompanied by an auxiliary head comprising a 2-layer multi-layer perceptron with a 128-dimensional embedding dimension. More details about the implementation can be found in Appendix I. COBRA is evaluated

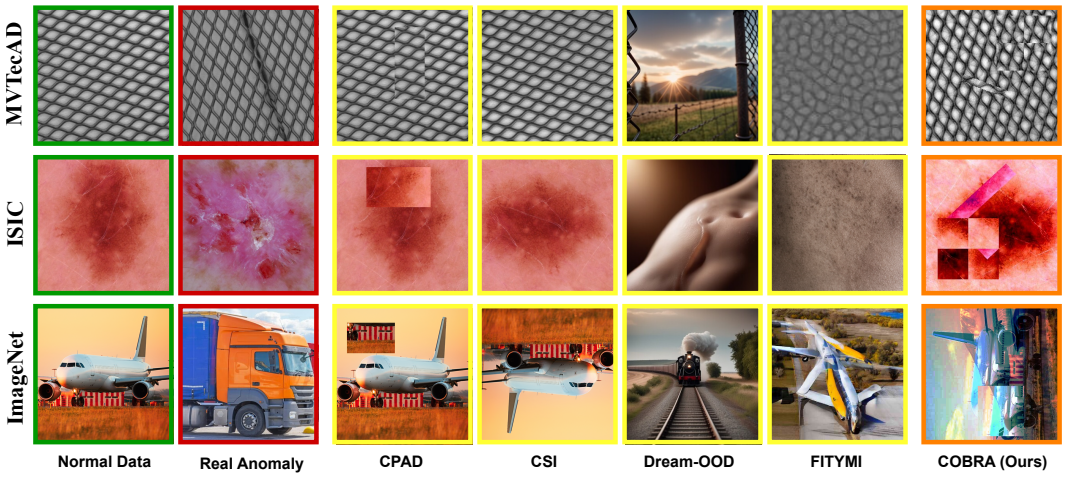

Figure 2: The figure highlights the challenges CPAD and CSI face in generating inncorrect anomalies due to the absence of a threshold. Techniques such as FITYMI and Dream-OOD, which generate anomalies from the embedding space of a pretrained model, typically lead to a loss of pixel-level detail and show biases towards the dataset used for pre-training (e.g., ImageNet). Such biases decrease their effectiveness on datasets not seen during pre-training, such as medical imaging datasets like ISIC. In contrast, COBRA, by adapting to the distribution of the normal dataset, efficiently crafts informative anomalies in the pixel space and utilizes a thresholding method to filter out incorrect anomalies, all **without** the need for any additional datasets.

Table 5: Comparison of performance of COBRA with replacing alternative anomaly synthesis methods, in terms of effectiveness for the robust AD task. *None* corresponds to a scenario where we neglect any pseudo-anomaly and adapt COBRA for that setting. Table cells present results in the 'Clean / PGD-1000' format. Experiments were performed in the one-class AD setup.

Dataset	Anomaly Craft Strategy							
	None	CPAD	CSI	GOE	VOS	FITYMI	Dream-OOD	Ours
MVTecAD	57.6 / 10.8	86.2 / 70.8	61.4 / 12.9	58.1 / 25.3	53.4 / 15.8	65.0 / 38.7	68.6 / 36.4	**89.1** / **75.1**
ImageNet	72.8 / 32.5	67.5 / 43.4	82.7 / 58.2	81.9 / 60.4	72.4 / 56.5	68.9 / 47.2	**87.3** / **64.1**	85.2 / 57.0
CIFAR10	78.6 / 50.3	69.4 / 53.8	82.9 / 60.7	**84.2** / 58.8	79.3 / 53.1	76.9 / 50.6	75.2 / 57.8	83.7 / **62.3**
FMnist	82.4 / 71.7	86.3 / 78.5	89.5 / 82.6	73.9 / 64.1	68.2 / 61.9	71.7 / 62.0	76.4 / 68.5	**93.1** / **89.6**
Average	72.8 / 41.3	77.3 / 61.6	79.0 / 53.1	74.5 / 52.1	68.3 / 47.3	70.6 / 50.3	76.9 / 56.7	**87.8** / **71.0**

using challenging datasets that includes both high- and low-resolution images. The high-resolution dataset comprises MVTecAD (7), VisA (77), CityScapes (29), ImageNet (30), ISIC2018 (31), and DAGM (78), while the low-resolution dataset includes SVHN (79), FMNIST (80), CIFAR10, CIFAR100, and MNIST. Further details can be found in Appendix L.

5 Ablation Study

Pseudo-anomaly Generating Strategy. In order to demonstrate the superiority of our strategy for pseudo-anomaly sample crafting, with other modules fixed, we replaced ours with alternative methods. We provided a brief description of alternative methods in Section 3.1. The results, which are presented in Table 5, along with a visualization comparison of samples in Figure 2, show the superiority of our effective synthesizer method. Notably, our strategy, without using any extra data, outperforms Dream-OOD with billions of sample complexity by a margin of 15%. In Appendix D.1, we further evaluate the quality of our generated data.

Adversarial Training Objective Function. We replaced our proposed loss function with various alternatives, such as classification (CLS), CL and Supervised CL. The results, detailed in Table 6, reveal that the COBRA loss function, by generating challenging intra- and inter-group adversarial examples during training, surpasses other alternatives significantly. L_{COBRA} outperforms CLS by

Table 6: Comparison of the performance of COBRA with alternative loss functions versus $\mathcal{L}_{\text{COBRA}}$, in terms of effectiveness for the robust AD task. Table cells present results in the 'Clean / PGD-1000' format. Experiments were performed in the one-class AD setup.

Dataset	Loss Function					
	$\mathcal{L}_{\text{CLS}}$	$\mathcal{L}_{\text{CL}}$	$\mathcal{L}_{\text{SupCL}}$	$\mathcal{L}_{\text{Opposite}}$	$\mathcal{L}_{\text{COBRA}}$	$\mathcal{L}_{\text{COBRA}} + \mathcal{L}_{\text{CLS}}$
MVTecAD	62.6 / 40.4	76.4 / 58.7	80.4 / 60.5	64.0 / 53.6	83.7 / 68.2	**89.1 / 75.1**
ImageNet	59.5 / 45.1	68.3 / 47.6	74.6 / 46.3	57.4 / 45.8	82.9 / 54.3	**85.2 / 57.0**
CIFAR10	62.6 / 49.6	67.9 / 54.3	74.2 / 53.8	65.9 / 52.4	78.5 / 61.0	**83.7 / 62.3**
FMnist	82.0 / 78.4	88.3 / 82.5	91.5 / 83.2	80.4 / 73.5	92.8 / 87.6	**93.1 / 89.6**
Average	66.7 / 53.3	75.2 / 60.8	80.4 / 60.9	66.9 / 56.3	84.5 / 67.7	**87.7 / 71.0**

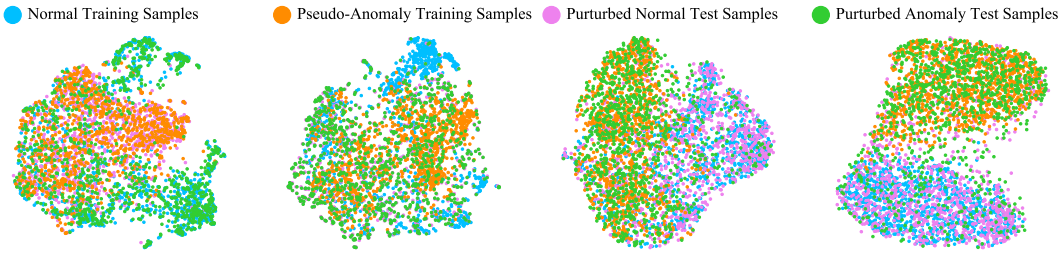

(a) CL (b) CLS (c) SupCLR (d) COBRA

Figure 3: UMAP visualization of features extracted by the encoder f, trained with various loss functions on the CIFAR-10 dataset, is presented in a one-class setup with the 'Automobile' class designated as the normal set. For this particular experiment, all elements except the loss function remain constant to ensure a fair comparison.

increasing normal distribution compactness provided by intra-group perturbations, and outperforms CL and SupCL by considering opposite pairs for increasing margins. As the results indicate, our perfomanc outperforms other loss functions by 11%. Additional ablation studies, experimental results including error bars, limitations, and qualitative visualizations are provided in the Appendix.

6 Conclusion

In conclusion, our work introduces COBRA, a novel and effective approach for enhancing AD methods' robustness against adversarial attacks. By leveraging a novel loss function inspired by contrastive learning and strategically crafting informative anomaly samples, COBRA achieves superior detection performance under both clean and adversarial evaluation conditions. We verify COBRA through comprehensive ablation experiments on its different components. Moreover, our extensive experiments across multiple challenging datasets, as well as under various strong attacks, confirm our method's effectiveness, setting a new benchmark for future research in reliable AD.

7 Limitations

Scope of Application In this study, we primarily focus on anomaly detection for texture-based defects, which are common in real-world applications such as industrial defect detection and medical image diagnosis. Specifically, while our experiments include one-class classification (semantic anomaly detection), our performance is more pronounced in texture-based anomaly detection. In semantic anomaly detection, normal samples and anomalous samples are semantically different.

Clean Performance This study aims to improve the adversarial detection performance of anomaly detection tasks. Despite significant improvements in adversarial detection, our clean performance lags behind existing state-of-the-art detection methods. The trade-off between clean and adversarial test performance is well-documented in the literature (70; 81; 18; 68; 82). Our work is also subject to such trade-offs. However, we have also provided results for scenarios where adversarial training is not performed.

REFERENCES

[1] Abhijit Bendale and Terrance Boult. Towards open world recognition. In *Proceedings of the IEEE Conference on Computer Vision and Pattern Recognition (CVPR)*, pages 1893–1902, 2015.

[2] Pramuditha Perera, Poojan Oza, and Vishal M Patel. One-class classification: A survey. *arXiv preprint arXiv:2101.03064*, 2021.

[3] Lukas Ruff, Robert Vandermeulen, Nico Goernitz, Lucas Deecke, Shoaib Ahmed Siddiqui, Alexander Binder, Emmanuel Müller, and Marius Kloft. Deep one-class classification. In *International conference on machine learning*, pages 4393–4402. PMLR, 2018.

[4] Jihoon Tack, Sangwoo Mo, Jongheon Jeong, and Jinwoo Shin. Csi: Novelty detection via contrastive learning on distributionally shifted instances. *Advances in neural information processing systems*, 33: 11839–11852, 2020.

[5] Liron Bergman, Niv Cohen, and Yedid Hoshen. Deep nearest neighbor anomaly detection. *arXiv preprint arXiv:2002.10445*, 2020.

[6] Tal Reiss, Niv Cohen, Liron Bergman, and Yedid Hoshen. Panda: Adapting pretrained features for anomaly detection and segmentation. In *Proceedings of the IEEE/CVF Conference on Computer Vision and Pattern Recognition*, pages 2806–2814, 2021.

[7] Paul Bergmann, Michael Fauser, David Sattlegger, and Carsten Steger. Mvtec ad–a comprehensive real-world dataset for unsupervised anomaly detection. In *Proceedings of the IEEE/CVF conference on computer vision and pattern recognition*, pages 9592–9600, 2019.

[8] Alex Krizhevsky, Geoffrey Hinton, et al. Learning multiple layers of features from tiny images. 2009.

[9] Mohammad Azizmalayeri, Arshia Soltani Moakhar, Arman Zarei, Reihaneh Zohrabi, Mohammad Manzuri, and Mohammad Hossein Rohban. Your out-of-distribution detection method is not robust! *Advances in Neural Information Processing Systems*, 35:4887–4901, 2022.

[10] Shao-Yuan Lo, Poojan Oza, and Vishal M Patel. Adversarially robust one-class novelty detection. *IEEE Transactions on Pattern Analysis and Machine Intelligence*, 2022.

[11] Jiefeng Chen, Yixuan Li, Xi Wu, Yingyu Liang, and Somesh Jha. Robust out-of-distribution detection for neural networks. *arXiv preprint arXiv:2003.09711*, 2020.

[12] Rui Shao, Pramuditha Perera, Pong C Yuen, and Vishal M Patel. Open-set adversarial defense. In *Computer Vision–ECCV 2020: 16th European Conference, Glasgow, UK, August 23–28, 2020, Proceedings, Part XVII 16*, pages 682–698. Springer, 2020.

[13] Rui Shao, Pramuditha Perera, Pong C Yuen, and Vishal M Patel. Open-set adversarial defense with clean-adversarial mutual learning. *International Journal of Computer Vision*, 130(4):1070–1087, 2022.

[14] Louis Béthune, Paul Novello, Thibaut Boissin, Guillaume Coiffier, Mathieu Serrurier, Quentin Vincenot, and Andres Troya-Galvis. Robust one-class classification with signed distance function using 1-lipschitz neural networks. *arXiv preprint arXiv:2303.01978*, 2023.

[15] Adam Goodge, Bryan Hooi, See Kiong Ng, and Wee Siong Ng. Robustness of autoencoders for anomaly detection under adversarial impact. In *Proceedings of the Twenty-Ninth International Conference on International Joint Conferences on Artificial Intelligence*, pages 1244–1250, 2021.

[16] Jiefeng Chen, Yixuan Li, Xi Wu, Yingyu Liang, and Somesh Jha. Atom: Robustifying out-of-distribution detection using outlier mining. In *Machine Learning and Knowledge Discovery in Databases. Research Track: European Conference, ECML PKDD 2021, Bilbao, Spain, September 13–17, 2021, Proceedings, Part III 21*, pages 430–445. Springer, 2021.

[17] Tao Bai, Jinqi Luo, Jun Zhao, Bihan Wen, and Qian Wang. Recent advances in adversarial training for adversarial robustness. *arXiv preprint arXiv:2102.01356*, 2021.

[18] Aleksander Madry, Aleksandar Makelov, Ludwig Schmidt, Dimitris Tsipras, and Adrian Vladu. Towards deep learning models resistant to adversarial attacks. *arXiv preprint arXiv:1706.06083*, 2017.

[19] Michael Glodek, Martin Schels, and Friedhelm Schwenker. Ensemble gaussian mixture models for probability density estimation. *Computational statistics*, 28:127–138, 2013.

[20] Shuo Chen, Gang Niu, Chen Gong, Jun Li, Jian Yang, and Masashi Sugiyama. Large-margin contrastive learning with distance polarization regularizer. In *International Conference on Machine Learning*, pages 1673–1683. PMLR, 2021.

[21] Xuxin Cheng, Bowen Cao, Qichen Ye, Zhihong Zhu, Hongxiang Li, and Yuexian Zou. Ml-lmcl: Mutual learning and large-margin contrastive learning for improving asr robustness in spoken language understanding. *arXiv preprint arXiv:2311.11375*, 2023.

[22] Yiwen Guo and Changshui Zhang. Recent advances in large margin learning. *IEEE Transactions on Pattern Analysis and Machine Intelligence*, 44(10):7167–7174, 2021.

[23] Ting Chen, Simon Kornblith, Mohammad Norouzi, and Geoffrey Hinton. A simple framework for contrastive learning of visual representations. In *Proceedings of the 37th International Conference on Machine Learning (ICML)*, pages 1597–1607. PMLR, 2020.

[24] Kaiming He, Haoqi Fan, Yuxin Wu, Saining Xie, and Ross Girshick. Momentum contrast for unsupervised visual representation learning. In *Proceedings of the IEEE/CVF conference on computer vision and pattern recognition*, pages 9729–9738, 2020.

[25] Jia Guo, Lize Jia, Weihang Zhang, Huiqi Li, et al. Recontrast: Domain-specific anomaly detection via contrastive reconstruction. *Advances in Neural Information Processing Systems*, 36, 2024.

[26] Tal Reiss and Yedid Hoshen. Mean-shifted contrastive loss for anomaly detection. *arXiv preprint arXiv:2106.03844*, 2021.

[27] Francesco Croce and Matthias Hein. Reliable evaluation of adversarial robustness with an ensemble of diverse parameter-free attacks. In *International conference on machine learning*, pages 2206–2216. PMLR, 2020.

[28] Ye Liu, Yaya Cheng, Lianli Gao, Xianglong Liu, Qilong Zhang, and Jingkuan Song. Practical evaluation of adversarial robustness via adaptive auto attack, 2022.

[29] Marius Cordts, Mohamed Omran, Sebastian Ramos, Timo Rehfeld, Markus Enzweiler, Rodrigo Benenson, Uwe Franke, Stefan Roth, and Bernt Schiele. The cityscapes dataset for semantic urban scene understanding. In *Proc. of the IEEE Conference on Computer Vision and Pattern Recognition (CVPR)*, 2016.

[30] Jia Deng, Wei Dong, Richard Socher, Li-Jia Li, Kai Li, and Li Fei-Fei. Imagenet: A large-scale hierarchical image database. In *2009 IEEE Conference on Computer Vision and Pattern Recognition*, pages 248–255. IEEE, 2009.

[31] Noel Codella, Veronica Rotemberg, Philipp Tschandl, M Emre Celebi, Stephen Dusza, David Gutman, Brian Helba, Aadi Kalloo, Konstantinos Liopyris, Michael Marchetti, et al. Skin lesion analysis toward melanoma detection 2018: A challenge hosted by the international skin imaging collaboration (isic). *arXiv preprint arXiv:1902.03368*, 2019.

[32] Jingkang Yang, Kaiyang Zhou, Yixuan Li, and Ziwei Liu. Generalized out-of-distribution detection: A survey. *arXiv preprint arXiv:2110.11334*, 2021.

[33] Lukas Ruff, Jacob R Kauffmann, Robert A Vandermeulen, Grégoire Montavon, Wojciech Samek, Marius Kloft, Thomas G Dietterich, and Klaus-Robert Müller. A unifying review of deep and shallow anomaly detection. *Proceedings of the IEEE*, 109(5):756–795, 2021.

[34] Shu Kong and Deva Ramanan. Opengan: Open-set recognition via open data generation. In *Proceedings of the IEEE/CVF International Conference on Computer Vision*, pages 813–822, 2021.

[35] Songqiao Han, Xiyang Hu, Hailiang Huang, Minqi Jiang, and Yue Zhao. Adbench: Anomaly detection benchmark. *Advances in Neural Information Processing Systems*, 35:32142–32159, 2022.

[36] Chun-Liang Li, Kihyuk Sohn, Jinsung Yoon, and Tomas Pfister. Cutpaste: Self-supervised learning for anomaly detection and localization. In *Proceedings of the IEEE/CVF Conference on Computer Vision and Pattern Recognition*, pages 9664–9674, 2021.

[37] Konstantin Kirchheim and Frank Ortmeier. On outlier exposure with generative models. In *NeurIPS ML Safety Workshop*, 2022.

[38] Hossein Mirzaei, Mohammadreza Salehi, Sajjad Shahabi, Efstratios Gavves, Cees GM Snoek, Mohammad Sabokrou, and Mohammad Hossein Rohban. Fake it till you make it: Near-distribution novelty detection by score-based generative models. *arXiv preprint arXiv:2205.14297*, 2022.

[39] Xuefeng Du, Yiyou Sun, Xiaojin Zhu, and Yixuan Li. Dream the impossible: Outlier imagination with diffusion models. *arXiv preprint arXiv:2309.13415*, 2023.

[40] Robin Rombach, Andreas Blattmann, Dominik Lorenz, Patrick Esser, and Björn Ommer. High-resolution image synthesis with latent diffusion models. In *Proceedings of the IEEE/CVF Conference on Computer Vision and Pattern Recognition*, pages 10684–10695, 2022.

[41] Christoph Schuhmann, Romain Beaumont, Richard Vencu, Cade Gordon, Ross Wightman, Mehdi Cherti, Theo Coombes, Aarush Katta, Clayton Mullis, Mitchell Wortsman, et al. Laion-5b: An open large-scale dataset for training next generation image-text models. *arXiv preprint arXiv:2210.08402*, 2022.

[42] Xuefeng Du, Zhaoning Wang, Mu Cai, and Yixuan Li. Vos: Learning what you don't know by virtual outlier synthesis. *arXiv preprint arXiv:2202.01197*, 2022.

[43] Hossein Mirzaei, Mohammad Jafari, Hamid Reza Dehbashi, Ali Ansari, Sepehr Ghobadi, Masoud Hadi, Arshia Soltani Moakhar, Mohammad Azizmalayeri, Mahdieh Soleymani Baghshah, and Mohammad Hossein Rohban. Rodeo: Robust outlier detection via exposing adaptive out-of-distribution samples. In *Forty-first International Conference on Machine Learning*, 2024.

[44] Yifei Ming, Ying Fan, and Yixuan Li. Poem: Out-of-distribution detection with posterior sampling. In *International Conference on Machine Learning*, pages 15650–15665. PMLR, 2022.

[45] Izhak Golan and Ran El-Yaniv. Deep anomaly detection using geometric transformations. *Advances in neural information processing systems*, 31, 2018.

[46] Dan Hendrycks, Mantas Mazeika, Saurav Kadavath, and Dawn Song. Using self-supervised learning can improve model robustness and uncertainty. *Advances in Neural Information Processing Systems*, 32, 2019.

[47] Kejiang Chen, Yuefeng Chen, Hang Zhou, Xiaofeng Mao, Yuhong Li, Yuan He, Hui Xue, Weiming Zhang, and Nenghai Yu. Self-supervised adversarial training. In *ICASSP 2020-2020 IEEE International Conference on Acoustics, Speech and Signal Processing (ICASSP)*, pages 2218–2222. IEEE, 2020.

[48] Dan Hendrycks, Mantas Mazeika, and Thomas Dietterich. Deep anomaly detection with outlier exposure. *arXiv preprint arXiv:1812.04606*, 2018.

[49] Leitian Tao, Xuefeng Du, Xiaojin Zhu, and Yixuan Li. Non-parametric outlier synthesis, 2023.

[50] Hongyi Zhang, Moustapha Cisse, Yann N Dauphin, and David Lopez-Paz. mixup: Beyond empirical risk minimization. *arXiv preprint arXiv:1710.09412*, 2017.

[51] Mehdi Noroozi and Paolo Favaro. Unsupervised learning of visual representations by solving jigsaw puzzles. In Bastian Leibe, Jiri Matas, Nicu Sebe, and Max Welling, editors, *Computer Vision – ECCV 2016*, pages 69–84, Cham, 2016. Springer International Publishing. ISBN 978-3-319-46466-4.

[52] Zhun Zhong, Liang Zheng, Guoliang Kang, Shaozi Li, and Yi Yang. Random erasing data augmentation. In *Proceedings of the AAAI Conference on Artificial Intelligence (AAAI)*, 2020.

[53] Golnaz Ghiasi, Yin Cui, Aravind Srinivas, Rui Qian, Tsung-Yi Lin, Ekin D Cubuk, Quoc V Le, and Barret Zoph. Simple copy-paste is a strong data augmentation method for instance segmentation. *arXiv preprint arXiv:2012.07177*, 2020.

[54] M. Eren Akbiyik. Data augmentation in training cnns: Injecting noise to images. *ArXiv*, abs/2307.06855, 2019. URL `https://api.semanticscholar.org/CorpusID:214522707`.

[55] Yann N. Dauphin Hongyi Zhang, Moustapha Cisse. mixup: Beyond empirical risk minimization. *International Conference on Learning Representations*, 2018. URL `https://openreview.net/forum?id=r1Ddp1-Rb`.

[56] Terrance DeVries and Graham W Taylor. Improved regularization of convolutional neural networks with cutout. *arXiv preprint arXiv:1708.04552*, 2017.

[57] Sangdoo Yun, Dongyoon Han, Seong Joon Oh, Sanghyuk Chun, Junsuk Choe, and Youngjoon Yoo. Cutmix: Regularization strategy to train strong classifiers with localizable features, 2019.

[58] Kihyuk Sohn, Chun-Liang Li, Jinsung Yoon, Minho Jin, and Tomas Pfister. Learning and evaluating representations for deep one-class classification. *arXiv preprint arXiv:2011.02578*, 2020.

[59] Dong Huk Park and Trevor Darrell. Novelty detection with rotated contrastive predictive coding. 2020.

[60] Puck de Haan and Sindy Löwe. Contrastive predictive coding for anomaly detection. *arXiv preprint arXiv:2107.07820*, 2021.

[61] Yannis Kalantidis, Mert Bulent Sariyildiz, Noe Pion, Philippe Weinzaepfel, and Diane Larlus. Hard negative mixing for contrastive learning. *Advances in Neural Information Processing Systems*, 33:21798–21809, 2020.

[62] Abhishek Sinha, Kumar Ayush, Jiaming Song, Burak Uzkent, Hongxia Jin, and Stefano Ermon. Negative data augmentation. In *International Conference on Learning Representations*, 2021. URL https://openreview.net/forum?id=Ovp8dvB8IBH.

[63] Yannis Kalantidis, Mert Bulent Sariyildiz, Noe Pion, Philippe Weinzaepfel, and Diane Larlus. Hard negative mixing for contrastive learning. In H. Larochelle, M. Ranzato, R. Hadsell, M.F. Balcan, and H. Lin, editors, *Advances in Neural Information Processing Systems*, volume 33, pages 21798–21809. Curran Associates, Inc., 2020. URL https://proceedings.neurips.cc/paper/2020/file/f7cade80b7cc92b991cf4d2806d6bd78-Paper.pdf.

[64] Atsuyuki Miyai, Qing Yu, Daiki Ikami, Go Irie, and Kiyoharu Aizawa. Rethinking rotation in self-supervised contrastive learning: Adaptive positive or negative data augmentation. In *Proceedings of the IEEE/CVF Winter Conference on Applications of Computer Vision (WACV)*, pages 2809–2818, January 2023.

[65] Zhaoyu Zhang, Yang Hua, Guanxiong Sun, Hui Wang, and Seán McLoone. Improving the leaking of augmentations in data-efficient gans via adaptive negative data augmentation. In *Proceedings of the IEEE/CVF Winter Conference on Applications of Computer Vision (WACV)*, pages 5412–5421, January 2024.

[66] Chengwei Chen, Yuan Xie, Shaohui Lin, Ruizhi Qiao, Jian Zhou, Xin Tan, Yi Zhang, and Lizhuang Ma. Novelty detection via contrastive learning with negative data augmentation. In Zhi-Hua Zhou, editor, *Proceedings of the Thirtieth International Joint Conference on Artificial Intelligence, IJCAI 2021, Virtual Event / Montreal, Canada, 19-27 August 2021*, pages 606–614. ijcai.org, 2021. doi: 10.24963/IJCAI.2021/84. URL https://doi.org/10.24963/ijcai.2021/84.

[67] Matan Jacob Cohen and Shai Avidan. Transformaly–two (feature spaces) are better than one. *arXiv preprint arXiv:2112.04185*, 2021.

[68] Ludwig Schmidt, Shibani Santurkar, Dimitris Tsipras, Kunal Talwar, and Aleksander Madry. Adversarially robust generalization requires more data. *Advances in neural information processing systems*, 31, 2018.

[69] David Stutz, Matthias Hein, and Bernt Schiele. Disentangling adversarial robustness and generalization. In *Proceedings of the IEEE/CVF Conference on Computer Vision and Pattern Recognition*, pages 6976–6987, 2019.

[70] Dimitris Tsipras, Shibani Santurkar, Logan Engstrom, Alexander Turner, and Aleksander Madry. Robustness may be at odds with accuracy. *arXiv preprint arXiv:1805.12152*, 2018.

[71] Karsten Roth, Latha Pemula, Joaquin Zepeda, Bernhard Schölkopf, Thomas Brox, and Peter Gehler. Towards total recall in industrial anomaly detection, 2021.

[72] Vitjan Zavrtanik, Matej Kristan, and Danijel Skočaj. Draem-a discriminatively trained reconstruction embedding for surface anomaly detection. In *Proceedings of the IEEE/CVF International Conference on Computer Vision*, pages 8330–8339, 2021.

[73] Hossein Mirzaei, Mohammad Jafari, Hamid Dehbashi, Zeinab Taghavi, Mohammad Sabokrou, and Mohammad Hossein Rohban. Killing it with zero-shot: Adversarially robust novelty detection. pages 7415–7419, 04 2024. doi: 10.1109/ICASSP48485.2024.10446155.

[74] Chuan Guo, Jacob Gardner, Yurong You, Andrew Gordon Wilson, and Kilian Weinberger. Simple black-box adversarial attacks. In *International Conference on Machine Learning*, pages 2484–2493. PMLR, 2019.

[75] Ian J Goodfellow, Jonathon Shlens, and Christian Szegedy. Explaining and harnessing adversarial examples. *arXiv preprint arXiv:1412.6572*, 2014.

[76] Xiaofeng Mao, Yuefeng Chen, Shuhui Wang, Hang Su, Yuan He, and Hui Xue. Composite adversarial attacks. *ArXiv*, abs/2012.05434, 2020. URL https://api.semanticscholar.org/CorpusID:228083968.

[77] Yang Zou, Jongheon Jeong, Latha Pemula, Dongqing Zhang, and Onkar Dabeer. Spot-the-difference self-supervised pre-training for anomaly detection and segmentation. In *European Conference on Computer Vision*, pages 392–408. Springer, 2022.

[78] Matthias Wieler, Tobias Hahn, and Fred A. Hamprecht. Weakly Supervised Learning for Industrial Optical Inspection, September 2007. URL `https://doi.org/10.5281/zenodo.8086136`. Acknowledgements The data was created by Matthias Wieler and Tobias Hahn. This work was conducted at the Robert Bosch Corporate Research department, Schwieberdingen, Germany. We also thank the participants in the contest, the participants of the symposium who helped finance the competition with their registration fees and the GNNS (German Chapter of the European Neural Network Society) for sponsoring the competition.

[79] Ian J Goodfellow, Yaroslav Bulatov, Julian Ibarz, Sacha Arnoud, and Vinay Shet. Multi-digit number recognition from street view imagery using deep convolutional neural networks. *arXiv preprint arXiv:1312.6082*, 2013.

[80] Han Xiao, Kashif Rasul, and Roland Vollgraf. Fashion-mnist: a novel image dataset for benchmarking machine learning algorithms. *arXiv preprint arXiv:1708.07747*, 2017.

[81] Hongyang Zhang, Yaodong Yu, Jiantao Jiao, Eric Xing, Laurent El Ghaoui, and Michael Jordan. Theoretically principled trade-off between robustness and accuracy. In *International conference on machine learning*, pages 7472–7482. PMLR, 2019.

[82] Aditi Raghunathan, Sang Michael Xie, Fanny Yang, John Duchi, and Percy Liang. Understanding and mitigating the tradeoff between robustness and accuracy. *arXiv preprint arXiv:2002.10716*, 2020.

[83] Jiawei Yu, Ye Zheng, Xiang Wang, Wei Li, Yushuang Wu, Rui Zhao, and Liwei Wu. Fastflow: Unsupervised anomaly detection and localization via 2d normalizing flows. *arXiv preprint arXiv:2111.07677*, 2021.

[84] Muhammad Ferjad Naeem, Seong Joon Oh, Youngjung Uh, Yunjey Choi, and Jaejun Yoo. Reliable fidelity and diversity metrics for generative models. 2020.

[85] Dan Hendrycks, Mantas Mazeika, and Thomas Dietterich. Deep anomaly detection with outlier exposure. *Proceedings of the International Conference on Learning Representations*, 2019.

A ALGORITHM BLOCK

Algorithm 1 Adversarially Robust Anomaly Detection through Spurious Negative Pair Mitigation

$\mathcal{T} \leftarrow$ {Color Jitter, Horizontal Flip, Grayscale, ...} ▷ Set of k light augmentations
$T \leftarrow$ {Rotation, Elastic, Distortion, ...} ▷ Set of k hard augmentations

function CLASSIFIER_GMM_TRAINER(training_data, T)
  $synthetic_data \leftarrow \{(T_i(\text{training_data}), i) \mid T_i \in T, i \in \text{range}(T)\}$ ▷ Create k-class cls dataset
  Train a k-class classifier C on $synthetic_data$
  $e_{train} \leftarrow C(\text{training_data})$ ▷ Obtain embeddings from the classifier
  Fit GMM on e_{train}
  $\lambda \leftarrow 0.05$
  return C, GMM, λ
end function

function $\Upsilon(X_{normal}, T, C, \text{GMM}, \lambda)$
  while $p_value > \lambda$ **do**
    $transforms_seq \leftarrow$ Sample a random sequence of transforms from T
    $x_{p-anomaly} \leftarrow transforms_seq(x_{normal})$ ▷ Apply hard transformations to create a pseudo-anomaly
    $e_{p-anomaly} \leftarrow C(x_{p-anomaly})$ ▷ Obtain embeddings from the classifier
    $p_value \leftarrow$ GMM.P_Value $(e_{p-anomaly})$ ▷ Compute P-Value of embeddings
  end while
  return $x_{p-anomaly}$
end function

function PSEUDO_ANOMALY_GENERATOR(X_{normal}, T, C, GMM, λ)
  $X_{p-anomaly} = \{\}$
  for x_{normal} **in** X_{normal} **do** ▷ iterate over batch of normal data
    $x_{p-anomaly} \leftarrow \Upsilon(X_{normal}, T, C, \text{GMM}, \lambda)$
    $X_{p-anomaly}$.Add($x_{p-anomaly}$)
  end for
  return $X_{p-anomaly}$ ▷ Return the generated pseudo-anomaly sample
end function

function ADVERSARIAL_TRAINING_COBRA(training_data, $\mathcal{F}, \mathcal{G}, \mathcal{H}, C$, GMM, λ)
  for $\mathcal{B}_{normal}$ **in** training_data **do**
    $\mathcal{B}_{p-anomaly} \leftarrow$ Pseudo_Anomaly_Generator($\mathcal{B}_{normal}$)
    $\mathcal{B} \leftarrow$ Concatenate($\mathcal{B}_{normal}, \mathcal{B}_{p-anomaly}$)
    $Y \leftarrow [0] \times \|\mathcal{B}_{normal}\| + [1] \times \|\mathcal{B}_{p-anomaly}\|$
    $\tau_1, \tau_2 =$ Sample tow random requence of transforms from $\mathcal{T}$
    $\mathcal{B}_{adv} \leftarrow \{\}$
    for x, y **in** $(\mathcal{B}, Y)$ **do**
      $x_1, x_2 \leftarrow \tau_1(x), \tau_2(x)$
      P(x_1), P(x_2) $\leftarrow \{x_2\}, \{x_1\}$
      N(x) $\leftarrow \{\tau_1(x') : x' \in \mathcal{B} \setminus \{x\}\} \cup \{\tau_2(x') : x' \in \mathcal{B} \setminus \{x\}\}$ ▷ N(x)=N(x_1)=N(x_2)
      $x_{adv} \leftarrow x + \text{argmax}_{\|\delta\| \leq \epsilon} [\mathcal{L}_{\text{COBRA}}(\mathcal{F}, \mathcal{G}; x + \delta) + \mathcal{L}_{\text{CLS}}(\mathcal{F}, \mathcal{H}; x + \delta, y)]$
      $\mathcal{B}_{adv}$.Add(x_{adv})
    end for
    $\mathcal{L} = 0$
    for x, x_{adv}, y **in** $(\mathcal{B}, \mathcal{B}_{adv}, Y)$ **do**
      $x_1, x_2 \leftarrow \tau_1(x), \tau_2(x)$
      P(x_1), P(x_2), P(x_{adv}) $\leftarrow \{x_2, x_{adv}\}, \{x_1, x_{adv}\}, \{x_1, x_2\}$
      N(x) $\leftarrow \{\tau_1(x') : x' \in \mathcal{B} \setminus \{x\}\} \cup \{\tau_2(x') : x' \in \mathcal{B} \setminus \{x\}\}$
        $\cup \{x'_{adv} : x'_{adv} \in \mathcal{B}_{adv} \setminus \{x_{adv}\}\}$
      $\mathcal{L}$ += $\mathcal{L}_{\text{COBRA}}(\mathcal{F}, \mathcal{G}; x) + \mathcal{L}_{\text{CLS}}(\mathcal{F}, \mathcal{H}; [x, x_{adv}], [y, y])$
    end for
    Update Networks($\mathcal{F}, \mathcal{G}, \mathcal{H}$) using $\mathcal{L}$
  end for
end function

function MAIN(epochs, training_data, $\mathcal{F}, \mathcal{G}, \mathcal{H}$)
  C, GMM, $\lambda \leftarrow$ Classifier_GMM_Trainer(training_data, T)
  for epoch **in** epochs **do**
    Adversarial_Training_COBRA(training_data, $\mathcal{F}, \mathcal{G}, \mathcal{H}, C$, GMM, λ)
  end for
end function

MAIN(epochs, training_data, $\mathcal{F}, \mathcal{G}, \mathcal{H}$)

B RELATED WORK

Previous AD Methods. Recent standard AD methods can be categorized into two types: transfer learning based and CL based methods. Transfer learning-based methods utilize a trained model on a large dataset as a backbone and leverage its rich features for the AD task. This approach is evident in methods including PANDA (6), Transformaly (67), Patchcore (71), and Fastflow (83). On the other hand, CL framework has demonstrated its superiority by extracting discriminative features, as showcased by CSI (4), MSAD (26), Recontrast (25), and Draem (72). Extending transfer learning based methods to an adversarial setting is not feasible because pre-trained features, which act as a key, are not robust, necessitating a new training paradigm. This limitation inspired us to adopt CL for adversarial training, which also aligns with the unlabeled nature of AD. There have been a few efforts to propose robust AD methods, including PrincipaLS (10), OCSDF (14), and APAE (15). However, their results on even tiny datasets are less than random detection. Details about each mentioned method can be found in Appendix C.

C DETAILS OF RELATED WORK

C.1 PREVIOUS AD METHODS

There has been some efforts to develope a robust AD method. PrincipaLS employs a novel latent space manipulation technique to adjust the representations of data point with optimizing a robustness criterion designed to minimize the model's sensitivity to adversarial perturbations. OCSDF leverages the Signed Distance Function to delineate the boundary of a data distribution. Through the employment of 1-Lipschitz neural networks, it adeptly approximates normality scores, thus enhancing robustness to adversarial perturbations. APAE introduces the approximate projection autoencoder as a defense mechanism, integrating gradient descent on latent embeddings and feature-weighting normalization to enhance detection robustness. it worth noting we exclude robust OOD detection from our experiments, where their method have been develpoed by relying on labels and could not extend to AD setup. ZARND a introduces a robust method enhancing anomaly detection by integrating robust features from pretrained models with nearest-neighbor algorithms. The approach significantly improves robustness against adversarial attacks, which traditionally degrade ND performance. By leveraging features from adversarially robust models and employing k-Nearest Neighbors (k-NN) for anomaly scoring.

C.2 AUXILIARY ANOMALY SAMPLE CRAFTING

Previous studies on anomaly generation often struggle with producing samples that are either too similar to normal instances (distant anomalies) or inadvertently create samples that still belong to the normal category. Conversely, many studies have underscored the benefit of using related auxiliary anomaly samples to enhance detector performance. In light of this, we have proposed COBRA, which, unlike its counterparts such as Dream-OOD, does not require an extra dataset and performs well in an unsupervised setting where labels for normal samples are not available.

COBRA aligns with the distribution of the normal dataset, effectively generating informative pseudo-anomalies within the pixel space. It employs a thresholding technique to sift out inaccuracies, all while obviating the need for supplementary datasets.

D DISTRIBUTION AWARE HARD TRANSFORMATION

In this section, we elaborate on the practical implementation details of our proposed pseudo-anomaly crafting strategy. As discussed in the main text of the paper, we set the hyperparameter β to 0.05. To assess the robustness of our model with respect to this parameter, we conducted extensive experiments over a broader range, specifically $[0.02, 0.20]$. The stability of our model's performance across this range is demonstrated in the experimental results (refer to Table 7). These findings underscore the robustness of our approach in handling varying hyperparameter settings without significant performance degradation.

Table 7: Performance of the model for different values of the hyperparameter β used in pseudo-anomaly crafting. Results are shown in each table cell as 'Clean/PGD-1000'. (Evaluations are done on CIFAR-10 and CIFAR-100 datasets under a PGD-1000 attack with $\epsilon = \frac{4}{255}$, and on other high-resolution datasets with $\epsilon = \frac{2}{255}$).

β	Datasets						
	cifar10	cifar100	MVTecAD	CityScapes	VisA	ISIC2018	DAGM
0.02	82.7 / 61.8	75.4 / 52.3	88.0 / 74.1	79.9 / 57.5	73.7 / 70.1	82.3 / 55.6	80.4 / 55.1
0.05	83.7 / 62.3	76.9 / 51.7	89.1 / 75.1	81.7 / 56.2	75.2 / 73.8	81.3 / 56.1	82.4 / 56.8
0.08	82.3 / 62.1	74.2 / 50.8	87.3 / 73.9	81.3 / 55.9	76.1 / 73.0	81.0 / 57.0	82.1 / 55.7
0.11	81.9 / 61.3	74.8 / 51.0	88.1 / 74.4	80.8 / 55.1	74.2 / 72.7	80.6 / 55.2	81.3 / 57.0
0.14	80.8 / 60.9	77.2 / 51.8	89.0 / 74.5	80.6 / 56.2	75.8 / 72.6	79.8 / 56.4	79.5 / 54.6
0.17	79.5 / 59.3	75.8 / 50.4	86.9 / 75.0	79.6 / 56.7	74.2 / 72.9	79.3 / 54.1	79.0 / 53.7
0.20	80.1 / 58.9	76.3 / 49.9	89.2 / 74.2	80.0 / 54.2	73.9 / 72.1	80.3 / 55.3	81.9 / 54.7

D.1 HARD TRANSFORMATION

We employed a series of hard transformations to create the T set. The transformations and their respective hyperparameters are as follows:

- **Jigsaw**: Images were divided into a 2x2 grid, and the tiles were randomly permuted. This transformation disrupts the spatial continuity of image features.
- **Random Erasing**: A random rectangular region in the image was erased, with a size proportional to the image area and an aspect ratio randomly chosen between 10% and 50%.
- **CutPaste**: A square region, with side length varying from 10% to 50% of the image width, was cut and pasted into a different location within the same image.
- **Rotation**: Images were rotated by a random angle within ± 90 degrees to introduce a moderate level of distortion.
- **Extreme Blurring**: Applied a Gaussian blur with a kernel size of up to 5% of the image width and a high variance ($\sigma = 2.5$), resulting in significant blurring.
- **Intense Random Cropping**: Random sections, sized between 50% and 80% of the original image size, were cropped to challenge the model with incomplete patterns.
- **Noise Injection**: Gaussian noise with a mean of 0 and a standard deviation of 0.1 was added to the images.
- **Extreme Cropping**: Cropped the image to retain only 40% to 60% of its original size, focusing on the center to ensure a significant deviation from the original distribution.
- **Mixup**: To create composite images that merge features from both source images in a more challenging manner, we combined pairs of images using a blending coefficient α, drawn from a Beta distribution Beta(α, α) with α set to 0.1. This lower value of α results in a higher variance of the mixing coefficients, producing images that are significantly more blended than with a higher α value. This aggressive mixing ensures the crafting of pseudo-anomaly samples.
- **Cutout**: Square regions with a side length of 25% of the image width were filled with a constant value to simulate occlusion.
- **CutMix**: Portions from one image were cut and pasted onto another, with the cut region's size approximately 20% of the image area.

Quality of Generated Abnormal Data. In Table 5 of our paper, we evaluated our crafting strategy by comparing it with alternative methods. Additionally, Figure 2 presents samples that visually compare our results with others. To address any concerns further, we employed the FID metric, which measures the distance from a normal distribution, as well as the DC metric (84) to assess diversity. A lower FID indicates that the crafted anomalies are more similar to normal instances, while a higher DC suggests greater diversity among the samples. Table 8 compares the quality of anomalies generated by our method with those from other alternatives, using the FID and DC metrics.

Table 8: Assessment of Generated Anomaly Data Quality Compared to Alternative Methods

Dataset	Metric	GOE	FITYMI	Dream-OOD	Dream-OOD	Ours
MVTecAD	FID ↓	245	163	227	227	129
	DC ↑	0.53	0.29	0.75	0.75	0.84
ImageNet	FID ↓	118	145	98	98	107
	DC ↑	0.64	0.38	0.87	0.87	0.58
CIFAR10	FID ↓	76	86	72	72	54
	DC ↑	0.45	0.36	0.56	0.56	0.72
FMNIST	FID ↓	42	37	64	64	32
	DC ↑	0.31	0.17	0.45	0.45	0.63
Average	FID ↓	120.3	107.8	115.3	115.3	**80.3**
	DC ↑	0.48	0.3	0.65	0.65	**0.69**

Table 9: clean training of COBRA

Methods	Datasets									
	CIFAR10	CIFAR100	MNIST	FMnist	SVHN	ImagenNet30	MVTechAD	VisA	DAGM	ISIC2018
COBRA	94.3	93.7	95.1	93.4	96.0	92.7	95.2	78.1	90.8	83.4

D.2 Positive Transformation

Consistent with the self-supervised learning literature (23; 24), we employ mild transformations that generate samples with minimal visual differences while fully preserving semantics. These include *color jitter, random grayscale conversion, and random cropping (cropping the image to retain 80% to 100% of its original size)*. These transformations are designed to subtly alter the appearance of images without changing their underlying content, thereby enabling the model to learn robust features that are invariant to minor perturbations.

E Additional Ablation Study

Here, we conduct further experiments to thoroughly evaluate COBRA across diverse settings, highlighting its key components and their substantial impact.

Clean Training In this scenario, we skipped adversarial training and instead trained COBRA with standard training, keeping all other components fixed. The results indicate that clean performance increased from **90.1%** to **94.1%**, demonstrating COBRA's superiority in various scenarios of training and evaluating. The results are presented in Table 9.

Anomaly Score Instead of utilizing our proposed Anomaly Score, we explored alternative approaches while keeping other components unchanged. Specifically, our default anomaly score is based on the similarity between a test sample and normal training samples. We substituted this anomaly score with logits provided by our binary classifier head. Specifically, the COBRA results reported in the main paper are based on the $A(x)$ anomaly score, which is defined as:

$$A(x) = -\max_{x^i \in D_{\text{train}}} \left\{ \langle \mathcal{G}(\mathcal{F}(x)), \mathcal{G}(\mathcal{F}(x^i)) \rangle \right\},$$

Instead, we replaced that with $A'(x) = p(\mathcal{H}(\mathcal{F}(x))|y = 1)$, which denotes the probability of belonging to the pseudo-anomaly class as assigned by the binary classifier head. Additionally, we considered $A(x) + A'(x)$ as another alternative. As the results presented in Table 10 demonstrate, all strategies achieve significant performance with minor differences.

Table 10: Ablation study on different score functions. Results are AUROC (%)

Dataset	Anomaly Score		
	$A(x) + A'(x)$	$A'(x)$	$A(x)$ (default)
MVTecAD	88.4 / 74.6	83.1 / 72.8	89.1 / 75.1
CIFAR10	81.9 / 60.2	76.1 / 55.7	83.7 / 62.3
FMNIST	89.6 / 87.4	88.5 / 84.8	93.1 / 89.6
CIFAR100	72.6 / 51.2	70.4 / 48.3	76.9 / 51.7

Table 11: C's performance in the AD task across various datasets.

Methods	Datasets									
	CIFAR10	CIFAR100	MNIST	FMnist	SVHN	ImagenNet30	MVTechAD	VisA	DAGM	ISIC2018
COBRA	77.1	72.4	86.0	83.6	74.7	80.3	75.2	64.9	78.5	73.2

Ablation Study on Distribution-Aware Hard Transformation
In this section, we utilize the feature extractor C as an anomaly detector to demonstrate that its learned features from the normal training set are meaningful and significantly surpass random detection, highlighting its role in crafting effective pseudo-anomaly samples. Results presented in Table 11.

Ablation Study on Thresholding
Here, while keeping all components of COBRA constant, we skip the thresholding strategy and instead use a random subset of hard transformations for crafting pseudo-anomaly samples. The results, indicated in Table 12, suggest that this approach leads to decreased performance due to the failure to filter incorrect pseudo-anomaly samples (those that still belong to the normal set).

Table 12: Impact of Skipping Thresholding on Pseudo-Anomaly Generation in COBRA

Methods	Datasets									
	CIFAR10	CIFAR100	MNIST	FMnist	SVHN	ImagenNet30	MVTechAD	VisA	DAGM	ISIC2018
COBRA	78.6 / 58.1	65.4 / 46.5	94.3 / 91.5	90.1 / 86.5	84.8 / 53.2	72.5 / 55.7	76.0 / 68.2	78.4 / 47.9	74.6 / 52.0	73.8 / 51.4

F ANALYZING COBRA'S STABILITY AND EFFECTIVENESS

Figure 4 represents COBRA's loss values and its detection performance at each epoch of training for both clean data and data subjected to PGD attack, demonstrating the stability of COBRA's loss function. The experiment was conducted in a one-class setup using the MVETEC-AD and FMNIST datasets. Note that the loss values have been normalized between 0 and 1, and the loss values for the PGD data are higher than those for the clean data. Despite this, the figure underscores the stability of our loss function, which remains consistent across different training conditions.

G A^3 TO ALL METHODS

Table 13: AUROC (%) of various methods for One Class AD methods under AutoAttack.

*These models are trained to be adversarially robust.

Dataset	Method									
	DeepSVDD	CSI	DN2	PANDA	MSAD	Transformaly	PatchCore	PrincipaLS*	OCSDF*	APAE*
CIFAR10	16.6	3.3	2.5	1.2	0.7	2.4	2.5	29.6	26.9	2.0
CIFAR100	14.3	1.2	0.7	1.1	10.7	7.3	3.5	24.6	19.8	0.9
MNIST	15.4	1.7	1.0	0.7	14.1	11.6	2.4	77.3	66.2	28.6
Fashion-MNIST	48.1	8.5	2.2	9.7	3.7	2.8	2.8	67.5	59.6	12.3
SVHN	4.3	0.8	0.2	0.4	0.1	0.2	1.1	8.9	6.1	0.3
ImageNet30	12.4	2.7	1.2	0.5	1.4	1.8	2.3	23.8	20.6	1.1

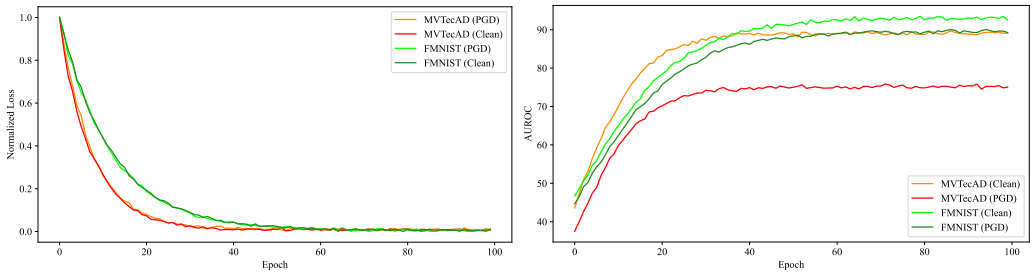

(a) Loss (b) AUC

Figure 4: This figure depicts COBRA's loss values and detection performance for each epoch of training on both clean data and data under PGD attack, demonstrating the stability of COBRA's loss function. The experiment was carried out in a one-class setup using the MVETEC-AD and FMNIST datasets.

Here, we present more detailed results of previous anomaly detection (AD) works and their performance under A^3 (See Table 13). Their respective performance against PGD-1000 attacks has been provided in the main paper.

H EVALUATING OUR MODEL UNDER VARIOUS ATTACKS WITH DIVERSE EPSILON VALUES

In this section, we evaluate our model's performance under adversarial attacks, specifically focusing on ℓ_∞ and ℓ_2 PGD attacks across various epsilon values. Table 14 presents the results for the ℓ_∞ PGD-1000 attacks, indicating that the model maintains strong accuracy for lower epsilon values, with some decline in performance observed as epsilon increases. Similarly, Table 15 illustrates the model's robustness under ℓ_2 PGD attacks, demonstrating consistent accuracy across lower epsilon values, with a gradual trend observed at higher epsilon values. These results highlight the model's resilience to adversarial attacks while also indicating areas for potential improvement.

Table 14: Evaluation of our model under various ℓ_∞ PGD-1000 attacks across different ϵ values. Although the model was trained using ℓ_∞ PGD-10 with $\epsilon = 2/255$ for high-resolution images and $\epsilon = 4/255$ for low-resolution images, the evaluation settings were modified to test its robustness against stronger attacks.

Epsilon	MVTec	VisA	ImageNet	CityScapes	ISIC2018	CIFAR10	FMNIST	Avg.
0	89.1	75.2	85.2	81.7	81.3	83.7	93.1	84.2
1/255	81.6	74.6	68.1	65.7	62.8	77.0	91.1	74.4
2/255	75.1	73.8	57.0	56.2	56.1	72.9	90.2	68.7
3/255	64.7	67.2	54.1	50.9	51.8	69.3	89.9	64.0
4/255	56.1	52.9	45.2	47.1	49.3	62.3	89.6	57.5
5/255	49.5	46.3	43.7	40.9	45.5	60.8	89.2	53.7
6/255	42.8	40.7	39.4	38.6	42.1	56.3	89.2	49.9
7/255	38.1	33.9	34.5	35.2	39.6	51.8	89.1	46.0
8/255	34.2	30.7	28.6	32.8	35.5	47.4	89.1	42.6

I IMPLEMENTATION DETAILS

We employ ResNet-18 as the foundational encoder network (f_θ), accompanied by an auxiliary head (g_ϕ) consisting of a 2-layer multi-layer perceptron with a 128-dimensional embedding. For optimization, COBRA is trained for 100 epochs using the LARS optimizer, with a weight decay of 1×10^{-6} and a momentum of 0.9. To schedule the learning rate, we adopt a linear warmup for the initial 10 epochs, gradually increasing the learning rate to 1.0. Subsequently, we use a cosine decay

Table 15: Evaluation of our model under various ℓ_2 PGD attacks across different ϵ values. Although the model was trained using ℓ_∞ PGD-10 with $\epsilon = 2/255$ for high-resolution images and $\epsilon = 4/255$ for low-resolution images, the evaluation settings were modified to test its robustness under stronger ℓ_2-norm adversarial attacks.

Epsilon	MVTec	VisA	ImageNet	CityScapes	ISIC2018	CIFAR10	FMNIST	Avg.
0	89.1	75.2	85.2	81.7	81.3	83.7	93.1	84.2
16/255	87.1	74.9	77.8	77.9	76.8	73.8	91.0	79.9
32/255	85.4	74.8	75.1	77.8	74.2	64.1	89.9	77.3
64/255	83.8	74.2	71.0	72.6	71.3	55.4	88.9	73.9
128/256	79.6	73.1	65.0	66.7	60.5	48.9	87.6	68.8

schedule without restarts. The batch size for COBRA is set to 128. Our experiments were conducted using NVIDIA GeForce RTX 3090 GPUs (24GB).

Training Computational Cost. COBRA comprises two main steps: (i) generating pseudo-anomaly samples from the normal training set, and (ii) adversarially training a model using both normal and crafted pseudo-anomalies. In this section, we analyze the complexity of these steps. Figure 5 illustrates that COBRA achieves significant performance with low complexity in terms of time. Please note that the training time shown in the figure is calculated for a single class of the dataset. In Table 16, we compare the time efficiency of our method, both with and without adversarial training, against other state-of-the-art methods across multiple datasets.

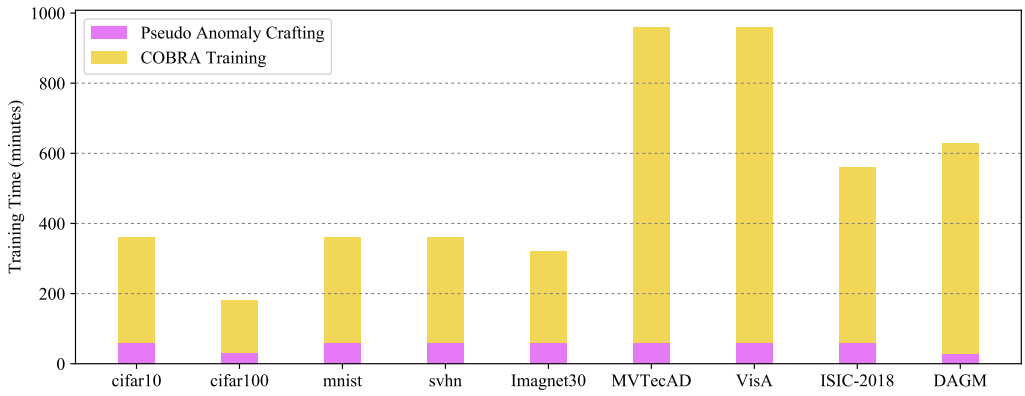

Figure 5: Computation cost

Table 16: Training Time Comparison (in hours) Across Different Methods and Datasets

Method	MVTecAD	VisA	CityScape	ImageNet
Transformaly	30h	70h	6h	200h
ReContrast	25h	60h	5h	180h
Ours (with adv. training)	95h	250h	20h	500h
Ours (without adv. training)	9h	23h	2h	70h

Evaluation of Computational Cost. After training, we freeze our model and extract features from the training samples to create an embedding bank, which maps images from high-dimensional spaces (e.g., (1000, 3, 224, 224)) to a lower-dimensional space (e.g., (1000, 256)). During inference, for each test sample, we compute its features using the frozen model and compare its similarity to the precomputed embedding bank. This process is computationally efficient since it operates with a frozen model and in a low-dimensional space. To the best of our knowledge, using similarity-based methods, such as k-NN in embedding spaces for detection tasks, is common and well-established in the literature (e.g., MSAD). Furthermore, we provide detailed computational time information,

excluding the time required for feature bank creation as it can be precomputed. The anomaly score computation times on a 3090 GPU, in comparison to other methods, are presented in Table 17, with results averaged over 100,000 inferences. For our model, embedding extraction takes 1-3 ms, matrix multiplication 1-2 ms, and finding the maximum value takes less than 1 ms.

Table 17: Per-Image Evaluation Time Comparison (in milliseconds) Across Different Methods

Metric	**CSI**	**MSAD**	**Transformaly**	**ReContrast**	**OCSDF**	**COBRA (Ours)**
Per-Image Eval Time	4 ms	4 ms	5 ms	5 ms	3 ms	4 ms

J PER-CLASS RESULTS

Anomaly detection evaluation scenarios can be categorized into one-class anomaly detection and unlabeled multi-class setups, as mentioned in the experiments section. In this section, we provide details of the one-class classification setup for COBRA on the reported dataset, as presented in Tables 18, 19.

.

Table 18: The detailed AUROC scores of the class-wise experiments for One-Class Anomaly Detection setting with PGD-1000 $\epsilon = \frac{4}{255}$ in CIFAR10, CIFAR100, MNIST, Fashion-MNIST, SVHN datasets.

(a) MNIST

Method	Attack	Class										Average
		0	1	2	3	4	5	6	7	8	9	
Ours	Clean	97.6	39.9	99.6	99.2	98.9	98.3	99.6	95.6	99.7	99.6	92.8
	BlackBox	92.4	99.6	98.9	95.1	97.5	94.6	99.1	96.9	96	97.2	96.8
	PGD-100	92.4	99.3	98.3	95.1	96.9	94.4	98.7	96.7	96	96.6	96.4
	A^3	91.7	98.3	97.8	94.3	94.5	94	97.3	94.3	95.1	94.4	95.2

(b) Fashion-MNIST

Method	Attack	Class										Average
		0	1	2	3	4	5	6	7	8	9	
COBRA	Clean	89.5	99.6	92.7	91.4	86.7	97.1	82.5	97	96.2	98.4	93.1
	BlackBox	88.7	99.5	85.8	85.7	83.3	95.3	82.6	97.9	92.6	97.8	90.9
	PGD-100	85.4	99	85.1	84.6	83	95.3	80.9	95.1	90.7	97.4	89.6
	A^3	83.7	96.5	85	83.9	81.7	93.5	77.2	91.5	87	93.6	87.4

(c) CIFAR10

Method	Attack	Class										Average
		0	1	2	3	4	5	6	7	8	9	
Ours	Clean	79.4	96.3	75.4	71.3	76	84.3	76.1	94.5	92.8	91.1	83.7
	BlackBox	75.9	96.1	75.2	68.4	73.4	84	74.2	92	89.9	89.8	81.8
	PGD-100	64.7	80.4	47.9	39.9	49.5	60.7	52.9	74.8	80.3	71.7	62.3
	A^3	64.5	77.7	46.6	39.8	48.8	58.3	50.1	72.9	80.3	68.7	60.7

(d) SVHN

Method	Attack	Class										Average
		0	1	2	3	4	5	6	7	8	9	
Ours	Clean	793.7	89.6	88.8	79.3	88.3	88.9	89.8	93.1	90.4	90.9	89.3
	BlackBox	88.8	88.9	85.7	75.2	83.7	84.1	86.9	90.5	89.8	89.9	86.4
	PGD-100	61.2	61.8	54.5	45.4	59.4	55.2	61	67.7	54.4	61.4	58.2
	A^3	60.1	61.6	52.4	43.6	56.6	55.6	59.7	65.3	52.4	58.7	56.7

(e) CIFAR100

Method	Attack	Class																				Average
		0	1	2	3	4	5	6	7	8	9	10	11	12	13	14	15	16	17	18	19	
Ours	Clean	68.9	73.1	79.4	71.9	84.24	70.1	79.5	72.3	71.7	85.4	83.34	78.8	80	57.5	80.4	69.6	62.5	92.4	88.9	88.5	76.9
	BlackBox	65.6	72.7	79	70.2	80.7	68.2	75.4	72.1	71.3	84.1	79.7	76.5	78.6	54.4	76.7	65.4	60.7	91.3	85	87.4	74.6
	PGD-100	43.6	51.2	47.8	51.2	57.2	44.5	55.3	38.5	40.2	70.4	72.4	50.2	48.7	29.6	50.7	39.9	36	75.5	63.5	69.3	51.7
	A^3	42.6	48.1	47.4	51.2	56.6	42.9	52.9	35.8	40.1	69.5	72.4	48.3	47.3	27.3	49.3	37.4	32.4	72.5	62.3	66.7	60.7

Table 19: The detailed AUROC scores of the class-specific experiments for One-Class Anomaly Detection setting with PGD-1000 $\epsilon = \frac{4}{255}$ in Imagenet30 dataset.

(a) ImageNet30

Method	Attack	Class										Average
		0	1	2	3	4	5	6	7	8	9	
Ours	Clean	74.9	98.1	99.7	73.5	83.4	96.7	93.2	83.3	82.7	74	85.2
	BlackBox	72.3	93.3	95.6	71.1	80.1	96	89.1	82.2	78.8	70.3	82.4
	PGD-100	35.8	90.9	96.7	46.4	36.3	86.3	60.9	55.7	38.3	24.4	57
	A^3	34.9	89.8	94.6	44.2	32.7	82.6	56.4	52.6	35.8	22.6	54.7

(b) ImageNet30

Method	Attack	Class										Average
		10	11	12	13	14	15	16	17	18	19	
Ours	Clean	96.9	90.1	93.3	82.1	94.6	62.8	98.2	58.5	89.4	54.7	85.2
	BlackBox	96	87.1	91.8	78.3	90.3	62.5	95.4	55.5	88.7	51.9	82.4
	PGD-100	71.3	62.8	75.5	36.6	76.6	16.4	88.1	17	58.5	24	57
	A^3	67.1	61.6	70.9	35.7	72.6	13.8	87.1	15.9	55.7	22.2	54.7

(c) ImageNet30

Method	Attack	Class										Average
		20	21	22	23	24	25	26	27	28	29	
Ours	Clean	95	88.1	97.2	96.5	80.2	69.2	83.5	92.9	78.3	93.7	85.2
	BlackBox	92.3	83.9	91.5	96.3	75.1	65.3	82.4	89.9	76.7	90.8	82.4
	PGD-100	77.9	44.8	90.8	79.1	39.2	40.6	32.2	78.1	41.3	86.5	57
	A^3	74.7	44.9	89.8	75.2	35.7	38.4	31.8	77.3	38.8	84.4	54.7

K ADVERSARIAL ATTACKS ADAPTATION

We evaluated COBRA's robustness against a variety of powerful attacks, including BlackBox, FGSM, CAA, AutoAttack, A^3, and PGD-1000. These attacks, originally designed to compromise classification tasks by exploiting the cross-entropy loss, were adapted for anomaly detection (AD) tasks, focusing on the anomaly scores of detector models. The aim was to generate perturbations that increase the anomaly score for normal test samples and decrease it for anomalous ones. As discussed in the preliminaries section, adapting AutoAttack (AA) (27) for AD tasks was particularly challenging. AutoAttack is an ensemble of different attack methods, such as FAB, multi-targeted FAB, Square Attack, APGDT, APGD with cross-entropy loss, and APGD with DLR loss. The main challenge in adaptation arises because attacks based on DLR loss assume the model's output includes at least three elements, an assumption valid for classification tasks on datasets with three or more classes but not applicable to AD tasks. Consequently, we replaced the DLR loss component in AutoAttack with a PGD attack. However, for the other attacks under consideration, no adjustments were necessary.

L DATASETS DETAILS

The MVTecAD is an industrial defect detection dataset used to evaluate AD methods. It consists of 4,096 normal and 1,258 anomaly samples, encompassing various types of texture defects. MVTecAD is under the CC-BY-NC-SA 4.0 license. VisA is another challenging dataset for industrial defect detection, comprising 9,621 normal and 1,200 anomaly samples. VisA is under the CC-BY 4.0 license. DAGM is a synthetic dataset created for defect detection on textured surfaces. To broaden the scope beyond traditional industrial scenarios, the Cityscapes dataset offers stereo videos from 50 cities, each meticulously annotated for 30 classes such as roads and buildings. We leverage this dataset by extracting 256x256 patches from its images to construct an anomaly detection dataset, focusing on the presence of anomaly objects within these patches. Anomaly classes encompass motorcycles, persons, riders, traffic signs, traffic lights, and bicycles, while other classes from Cityscapes are considered normal. Their code is released under the MIT license. Additionally, ISIC2018 is a skin disease dataset, available as task 3 of the ISIC2018 challenge. It contains seven classes. NV (nevus) is taken as the normal class, and the rest of the classes are taken as anomalies, following. The training set contains 6,705 normal images. The ISIC dataset is available under CC-BY-NC license. Furthermore, we utilize ImageNet30 (46), an anomaly detection benchmark that selects 30 classes from ImageNet and employs a one-versus-rest setup for anomaly detection. This dataset is freely available to researchers for non-commercial use.

M DETAILED RESULTS

The figure presents the standard deviation and mean of COBRA (a specific algorithm or method) calculated over 5 separate runs for each experiment. This comprehensive data collection and analysis underscore the reliability and consistency of our experimental results. By reporting both the mean and standard deviation, we provide a clear depiction of the average performance and the variability, ensuring that the performance of COBRA is not only robust but also consistently reproducible across multiple trials.

Table 20: The standard deviation and mean of COBRA across 5 runs of each experiment are reported, demonstrating the consistency of our results.

Statistics	Eval Type	Datasets									
		CIFAR10	CIFAR100	MNIST	FMNIST	SVHN	ImageNet	VisA	CityScapes	DAGM	ISIC2018
Mean ± STD	Clean	83.7 ± 0.52	76.9 ± 0.81	92.8 ± 0.47	93.1 ± 0.56	89.3 ± 0.39	85.2 ± 1.21	75.2 ± 1.03	81.7 ± 0.97	82.4 ± 0.87	81.3 ± 0.74
	Adv	62.3 ± 0.73	51.7 ± 0.91	96.4± 0.86	89.6 ± 0.91	58.2 ± 0.62	57.0 ± 1.41	73.8 ± 1.17	56.2 ± 1.31	56.8 ±	56.1 ± 1.42

N SUPPLEMENTARY METRICS FOR COBRA ASSESSMENT

We found the Area Under the Receiver Operating Characteristic curve (AUROC) to be the most widely accepted and utilized metric. To further our exploration, we have provided additional results

using two supplementary metrics—AUPR and FPR95%—which have been utilized in some previous works (85). In the table 21, we compare COBRA against TRANSFORMALY and ZARND, a recent detection method, using these metrics. FPR95% represents the false positive rate when 95% of the outliers are correctly detected; a lower FPR95% signifies better performance. Both AUROC and AUPR summarize a detection method's performance over various thresholds. Specifically, AUROC indicates the likelihood that an outlier is ranked higher in anomaly score compared to an in-distribution sample. Hence, higher AUROC and AUPR values denote superior performance, with an uninformative detector scoring an AUROC of 50%. To address the reviewer's concerns, we will consider including AUPR and FPR95% along with AUROC in our final manuscript.

Table 21: Methods and Metrics Comparison Across Different Datasets

Methods	**Metric**	**MVTec**	**VisA**	**ImageNet**	**CityScapes**	**ISIC2018**	**CIFAR10**	**FMNIST**
Transformaly	AUROC ↑	88.5/2.2	85.5/0.0	99.0/2.9	87.4/4.5	86.6/3.9	98.3/3.7	94.4/7.4
	AUPR ↑	85.6/3.9	83.7/4.1	94.1/2.3	86.0/2.6	83.5/2.8	99.6/1.4	98.2/0.0
	FPR95% ↓	41.6/99.7	26.7/98.9	2.6/99.1	35.7/97.9	28.4/98.0	8.4/99.6	9.5/95.4
ZARND	AUROC ↑	71.6/30.1	71.8/24.9	96.4/27.4	75.9/28.6	70.2/14.6	89.7/56.0	95.0/82.3
	AUPR ↑	73.5/28.7	69.8/20.1	90.1/29.8	72.1/26.5	73.6/16.4	85.5/52.3	92.5/80.0
	FPR95% ↓	41.2/69.2	44.1/73.9	7.3/64.8	40.1/66.4	26.8/75.3	26.4/55.9	9.6/23.3
COBRA (Ours)	AUROC ↑	89.1/75.1	75.2/73.8	85.2/57.0	81.7/56.2	81.3/56.1	83.7/62.3	93.1/89.6
	AUPR ↑	91.7/71.9	78.6/70.3	88.9/61.2	85.6/62.1	87.6/59.8	84.7/65.7	95.1/89.8
	FPR95% ↓	18.5/36.8	35.8/38.7	24.9/54.7	29.3/55.0	30.1/52.7	26.4/43.9	6.7/17.3

O SOCIAL IMPACTS

Robust anomaly detection is crucial across many safety-critical domains like security, healthcare, finance, and manufacturing to identify potential threats, diseases, fraud or system faults before they cause harm. However, existing machine learning-based anomaly detectors are vulnerable to adversarial attacks that can make them miss anomalies or falsely flag normal data. Our work on COBRA presents a significant step towards developing reliable and robust anomaly detection systems resilient to adversarial conditions. By learning representations inherently robust to input perturbations and distribution shifts, COBRA enables safer anomaly detection deployment in security-sensitive areas where an adversary may attempt evasion. Notably, COBRA achieves high robustness without requiring anomaly data during training, valuable when such data is limited due to privacy/safety concerns. Overall, we believe COBRA importantly enhances the safety and reliability of anomaly detection systems. However, this powerful technology must be responsibly developed and deployed with technical safeguards, policy measures and institutional controls to maximize societal benefit while mitigating potential misuse risks. We advocate future work exploring robust machine learning trustworthy real-world deployment.